

Investigating the Potential of Electro-Coagulation and Forward  
Osmosis in Water Recovery from Non-Oily Wastewater Streams  
of Petro-chemical Industry



By

Kanwal Anwar

(Registration No: 00000361831)

Institute of Environmental Sciences and Engineering (IESE)

School of Civil and Environmental Engineering (SCEE)

National University of Sciences & Technology (NUST)

Islamabad, Pakistan

(2024)

Investigating the Potential of Electro-Coagulation and Forward  
Osmosis in Water Recovery from Non-Oily Wastewater Streams  
of Petro-chemical Industry



By

Kanwal Anwar

(Registration No: 00000361831)

A thesis submitted to the National University of Sciences and Technology, Islamabad,

in partial fulfillment of the requirements for the degree of

Master of Science in  
Environmental Engineering

Supervisor: Dr. Sher Jamal Khan

Co-Supervisor: Dr. Muhammad Saqib Nawaz

Institute of Environmental Sciences and Engineering (IESE)

School of Civil and Environmental Engineering (SCEE)

National University of Sciences & Technology (NUST)

Islamabad, Pakistan

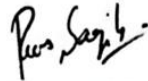
THESIS ACCEPTANCE CERTIFICATE

Certified that final copy of MS Thesis written by Ms. Kanwal Anwar (Registration No. 00000361831), of SCEE IESE has been vetted by the undersigned, found complete in all respects as per NUST Statutes/ Regulations/ Masters Policy, is free of plagiarism, errors, and mistakes and is accepted as partial fulfillment for award of Master's degree. It is further certified that necessary amendments as pointed out by GEC members and evaluators of the scholar, have also been incorporated in the said thesis.

Signature: 


Name of Supervisor Dr. Sher Jamal Khan

Date: 22-11-2024

Signature: 

Name of Co-Supervisor Dr. Muhammad Saqib Nawaz

Date: 22-11-2024

Signature (HOD): 

Date: 22-11-2024

Signature (Principal & Dean SCEE) 

Date: 28 NOV 2024 **PROF DR MUHAMMAD IRFAN**  
Principal & Dean  
SCEE, NUST

**CERTIFICATE OF APPROVAL**

This is to certify that research work presented in this thesis, titled “Investigating the Potential of Electro-Coagulation and Forward Osmosis in Water Recovery from Non-Oily Wastewater Streams of Petro-chemical Industry ” was conducted by Ms. Kanwal Anwar under the supervision of Dr. Sher Jamal Khan.



No part of this thesis has been submitted anywhere else for any other degree. This thesis is submitted to the SCEE (IESE) in partial fulfillment of the requirements for the degree of Master of Engineering in field of Environmental Engineering, School of Civil and Environmental Engineering, National University of Sciences and Technology, Islamabad.

Student Name: Kanwal Anwar

Signature 

**Guidance and Examination Committee:**

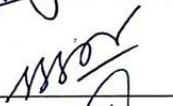
- a) Dr Muhammad Arshad
- b) Dr Musharib Khan

Signature   
Signature 

**Supervisor:** Dr Sher Jamal Khan

Signature 


**Head of Department:**

Signature 

**Associate Dean:** Dr Muhammad Arshad

Signature  **PROF DR MUHAMMAD ARSHAD**  
Associate Dean SCEE (IESE)  
SCEE, NUST H-12, Islamabad

**Principal & Dean SCEE**

Signature   
**PROF DR MUHAMMAD IRFAN**  
Principal & Dean  
SCEE, NUST

### Author's Declaration

I, **Kanwal Anwar** , hereby state that my PhD thesis titled “**Investigating the Potential of Electro-Coagulation and Forward Osmosis in Water Recovery from Non-Oily Wastewater Streams of Petro-chemical Industry**” is my own work and has not been submitted previously by me for taking any degree from National University of Sciences and Technology (NUST), Islamabad, or anywhere else in the country / world.

At any time if my statement is found to be incorrect even after my Graduation, the university has the right to withdraw my MS degree.

Dated: 21-11-2024

Signature: \_\_\_\_\_




Name of Student: Kanwal Anwar

## Plagiarism Undertaking

I solemnly declare that research work presented in the thesis titled “**Investigating the Potential of Electro-Coagulation and Forward Osmosis in Water Recovery from Non-Oily Wastewater Streams of Petro-chemical Industry**” is solely my research work with no significant contribution from any other person. Small contribution/help wherever taken has been duly acknowledged and that complete thesis has been written by me.

I understand the zero tolerance policy of the HEC and that of National University of Sciences and Technology (NUST), Islamabad, towards plagiarism. Therefore I, as an Author of the above titled thesis declare that no portion of my thesis has been plagiarized and any material used as reference is properly referred / cited.

I undertake that if I am found guilty of any formal plagiarism in the above titled thesis even after award of PhD degree, the University reserves the rights to withdraw / revoke my PhD degree and that HEC and the University has the right to publish my name on the HEC / University Website on which names of students are placed who submitted plagiarized thesis.

Student/ Author Signature:   
Name: Kanwal Anwar  
Date: 21-11-2024

## **DEDICATION**

To my beloved parents,

I would like to extend my special thanks to my parents for their constant support, love, and belief in me during my academic accomplishments. That is why in the moments of failure and in the moments of success, you are the one who encourages me and gives strength to work, to strive for the best and to pinch for the dreams.

This thesis is for you both, Ami and Abu, my source of strength. That your love has been my inspiration in moments of difficult times of life to give me the strength to do my best in any endeavor.

## **ACKNOWLEDGEMENTS**

Firstly, I express my gratitude to the Almighty Allah, the most gracious and beneficent, for providing me the opportunity to do an MS degree and for bringing patience and courage during the research work. This dissertation could not have been possible without the prayers, understanding, love, and support of my family, especially my parents.

It is my pleasure and privilege to acknowledge the support of my supervisor, Dr. Sher Jamal Khan, for the outstanding leadership and support he exhibited throughout my research. I appreciate his support in my research and thesis writing. I could not have imagined having a better advisor and mentor for my MS thesis than him. I want to express my appreciation to my co-supervisor, Dr. Muhammad Saqib Nawaz, for his guidance and help in this study. I am also thankful to him for his prompt and efficient reply to all the questions and inquiries I have raised during my research period. I would like to thank Dr. M. Arshad and Dr. Musharib Khan as my GEC for their constant support and constructive comments.

I also would like to thank the IESE's faculty, staff, and fellow classmates for their support. To my dear and precious friends and family, I can simply say that I am grateful. To the dear parents, I owe the most, Ammi and Abu, your constant support has been my biggest strength.



# TABLE OF CONTENTS

<b>ACKNOWLEDGEMENTS</b>	<b>VIII</b>
<b>TABLE OF CONTENTS</b>	<b>IX</b>
<b>LIST OF TABLES</b>	<b>XII</b>
<b>LIST OF FIGURES</b>	<b>XIII</b>
<b>LIST OF EQUATIONS</b>	<b>XIV</b>
<b>SYMBOLS, ABBREVIATIONS AND ACRONYMS</b>	<b>XV</b>
<b>ABSTRACT</b>	<b>XVI</b>
<b>CHAPTER 1: INTRODUCTION</b>	<b>1</b>
1.1 Background	1
1.2 Problem Statement	2
1.3 Significance and Novelty	3
1.4 Research Objectives	4
<b>CHAPTER 2: LITERATURE REVIEW</b>	<b>5</b>
2.1 Water Scarcity as a Global Issue	5
2.2 Water Consumption in the Petrochemical Sector	6
2.2.1 Drilling Processes	6
2.2.1.1 Drilling Fluid Composition	6
2.2.1.3 Pressure Control and Formation Stability	7
2.2.2 Refining Processes	7
2.2.2.4 Desalting and Contaminant Removal	8
2.3 Characteristics of Refinery Petrochemical Wastewater	8
2.4 Need for Wastewater Reuse	10
2.4.1 Water Scarcity	10
2.4.2 Environmental Protection	10
2.4.3 Regulatory Requirements	10
2.4.4 Economic Benefits	10
2.4.5 Resource Recovery	11
2.5 Existing Treatment Methods	11
2.5.1 Physical Treatment Methods	11
2.5.1.1 Gravity Separation	11
2.5.1.2 API	11
2.5.1.3 Dissolved Air	12
2.5.1.6 Centrifugation	13
2.5.2 Chemical Treatment Methods	13
2.5.2.1 Coagulation and Flocculation	13
2.5.2.2 Oxidation	13

2.5.2.3 pH Adjustment	14
2.5.3 Advanced Treatment Methods	14
2.5.3.1 Membrane Filtration	14
<b>2.6 Forward Osmosis (FO)</b>	<b>15</b>
2.6.1 Operation	15
2.6.2 Mechanism of FO	15
2.6.3 Use of TEAB in petro-chemical industry	16
2.6.4 Advantages of FO	18
2.6.5 Challenges of FO	18
2.6.6 Key Factors Contributing to Fouling in FO	20
<b>2.7 Electrocoagulation (EC)</b>	<b>21</b>
2.7.1 Operation	21
2.7.2 Mechanism of EC	21
2.7.3 Operational Parameters Affecting EC	23
2.7.4 Advantages of EC	25
2.7.5 Challenges of EC	25
<b>CHAPTER 3: METHODOLOGY</b>	<b>27</b>
<b>3.1 Characterization of synthetic wastewater</b>	<b>27</b>
<b>3.2 Draw Solution</b>	<b>29</b>
3.2.1 TEAB	30
3.2.2 Properties	30
<b>3.3 Description of Experimental Setup</b>	<b>30</b>
3.3.1 Membrane Specifications	30
<b>3.4 FO Batch Study</b>	<b>31</b>
<b>3.5 EC Batch Study</b>	<b>32</b>
<b>3.6 EC-FO Semi-Continuous Study</b>	<b>34</b>
<b>3.7 Analytical Methods</b>	<b>35</b>
3.7.1 Calculation of Water Flux and Reverse Solute Flux	35
3.7.2 Analysis of Sulfates, Calcium, Magnesium, Total Hardness, and pH	36
<b>3.8 Membrane Characterization</b>	<b>36</b>
3.8.1 SEM-EDX Analysis	37
3.8.2 Fourier Transform Infrared (FTIR) Analysis	37
3.8.3 Membrane Cleaning	38
<b>CHAPTER 4: RESULTS AND DISCUSSIONS</b>	<b>39</b>
<b>4.1 Effect of Cross Flow Velocity and Temperature</b>	<b>39</b>
4.1.1 SEM & EDX Analysis	43
4.1.2 FTIR Analysis	45
<b>4.2 Sulfate Removal via EC</b>	<b>47</b>
4.2.1 Effect of Current on Sulfate Removal with Stainless Steel Electrodes	47
4.2.2 Effect of Current on Sulfate Removal with Aluminium Electrodes	48
4.2.3 Effect of Current on Sulfate Removal with Aluminium Electrodes in Mono-Polar Parallel Arrangement	50
4.2.4 Effect of Bipolar Arrangement on Sulfate Removal at 1000 mA	52
<b>4.3 Removal of Ca, Mg, Sulfates, and Total Hardness</b>	<b>54</b>
4.3.1 Removal of Ca, Mg, Sulfates, and Total Hardness at 1500mA by using MP-S54	

4.3.2	Removal of Ca, Mg, Sulfates, and Total Hardness at 3000mA by using MP-P55	
4.3.3	Removal of Ca, Mg, Sulfates, and Total Hardness at 1000mA by using BP-S	57
4.3.4	Impact of Residence time on pH	58
4.3.5	Electrode Consumption in EC	60
4.3.6	Energy Consumption in EC	61
<b>4.4</b>	<b>Impact of Pre-Treatment on FO Flux</b>	<b>62</b>
<b>4.5</b>	<b>Flux Comparison for New Membrane, Chemical Cleaning, and Physical Cleaning</b>	<b>63</b>
<b>4.6</b>	<b>Comparative Analysis of Wastewater and Treated Wastewater Parameters</b>	<b>64</b>
<b>4.7</b>	<b>Semi Continuous EC-FO</b>	<b>67</b>
<b>CHAPTER 5: CONCLUSIONS AND RECOMMENDATIONS</b>		<b>69</b>
<b>5.1</b>	<b>Conclusion</b>	<b>69</b>
<b>5.2</b>	<b>Recommendations</b>	<b>70</b>
<b>REFERENCES</b>		<b>71</b>

## LIST OF TABLES

<b>Table 2.1:</b> Characteristics of real wastewater .....	9
<b>Table 3.1:</b> Composition of synthetic final non-oily stream .....	29
<b>Table 4.1:</b> Summary of 20 hrs batch experiments to assess the system performance .....	41
<b>Table 4.2:</b> Electrode Consumption in EC .....	60
<b>Table 4.3:</b> Energy Consumption in EC .....	62
<b>Table 4.4:</b> Comparative analysis of wastewater and treated wastewater parameters .....	66

## LIST OF FIGURES

<b>Figure 2.1:</b> Electric arrangement in electro-coagulation .....	25
<b>Figure 3.1:</b> Wastewater Generation Scheme.....	28
<b>Figure 3.2:</b> FO batch setup (1) Level sensor (2) Hanna EC Meter (3) Temperature sensor (4) Data logger (5) Feed solution (6) Hot plate stirrer (7) Peristaltic pump (8) Membrane module (9) Draw solution (10) Weighing balance .....	32
<b>Figure 3.3:</b> EC Batch Setup (1) Electrodes (2) DC supply (3) HANNA EC Meter (4) EC chamber (5) pH meter .....	33
<b>Figure 3.4:</b> Electro-coagulation samples stored for analysis .....	34
<b>Figure 3.5:</b> Schematic Diagram of Electro-Coagulation and Forward Osmosis .....	35
<b>Figure 4.1:</b> Flux at different Cross Flow Velocities at 30°C .....	40
<b>Figure 4.2:</b> Flux at different FS temperature at 8 cm/sec cross flow velocity .....	42
<b>Figure 4.3:</b> SEM-EDX analysis of AL of (a) CFV (FS = 8cm/s, DS = 8cm/s @ FS = 25°C, DS = 25°C) (b) CFV (FS = 16cm/s, DS = 8cm/s @ FS = 25°C, DS = 25°C) (c) CFV (FS = 24cm/s, DS = 8cm/s @ FS = 25°C, DS = 25°C) (d) CFV (FS = 8cm/s, DS = 8cm/s @ FS = 40°C, DS = 25°C) (e) CFV (FS = 8cm/s, DS = 8cm/s @ FS = 50°C, DS = 25°C).....	44
<b>Figure 4.4:</b> FTIR Analysis of active layers of (a) pristine membrane (b) CFV (feed solution = 8cm/s, draw solution = 8cm/s) (c) CFV (feed solution = 16cm/s, draw solution = 8cm/s) (d) CFV (feed solution = 24cm/s, DS = 8cm/s) (e) Temperature (feed solution = 40°C, draw solution = 30°C ) (f) (feed solution = 50°C, DS = 30°C ) .....	46
<b>Figure 4.5:</b> Effect of current on sulfate removal with stainless steel electrodes with MP-S .....	48
<b>Figure 4.6:</b> Effect of current on sulfate removal with aluminium electrodes with MP-S .....	49
<b>Figure 4.7:</b> Effect of current on sulfate removal with aluminium electrodes with MP-P .....	51
<b>Figure 4.8:</b> Effect of bi-polar series arrangement on sulfate removal at 1000 mA .....	53
<b>Figure 4.9:</b> Removal of Ca, Mg, Sulfates, and Total Hardness at 1500mA by using.....	55
<b>Figure 4.10:</b> Removal of Ca, Mg, Sulfates, and Total Hardness at 3000mA by using....	56
<b>Figure 4.11:</b> Removal of Ca, Mg, Sulfates, and Total Hardness at 1000mA by using....	58
<b>Figure 4.12:</b> Impact of Residence time on pH .....	59
<b>Figure 4.13:</b> Impact of Pre-Treatment by electro-coagulation on FO flux .....	63
<b>Figure 4.14:</b> Flux comparison for new membrane, chemical cleaning, and physical cleaning .....	64
<b>Figure 4.15:</b> Semi Continuous EC-FO.....	68

## LIST OF EQUATIONS

<b>Equation 4.1:</b> Electrode Consumption in EC .....	61
<b>Equation 4.2:</b> Energy Consumption in EC .....	62

## **SYMBOLS, ABBREVIATIONS AND ACRONYMS**

CFV	Cross Flow Velocity
CMC	Critical Micelle Concentration
DS	Draw Solution
EC	Electro-Coagulation
FO	Forward Osmosis
FS	Feed Solution
FTIR	Fourier Transform Infrared
GMH	Grams per meter square per hour
ICP	Internal Concentration Polarization
LMH	Litre per meter square per hour
RSF	Reverse Solute Flux
SDFO	Surfactant Driven Forward Osmosis
TEAB	Tetra Ethyl Ammonium Bromide
ZLD	Zero Liquid Discharge

## ABSTRACT

**Keywords:** Bi-polar series; Current Density; Energy Consumption; Membrane scaling

This study focuses on the treatment of the final non-oily wastewater stream originating from an oil refinery and processing site. Pre-treatment using electro-coagulation and main treatment/water recovery using forward osmosis (FO) is recommended. Firstly, the FO batch experiments were conducted with 0.75 M tetraethyl ammonium bromide (TEAB) as the surfactant draw solution and final non-oily stream as the feed solution. The feed solution cross flow velocity of 8 cm/s with operating temperature of 30 °C achieved the highest permeate flux of 7 L/m<sup>2</sup>/h, accompanied by a reverse solute flux of 0.19 g/m<sup>2</sup>/h. The FO membrane remained chemically stable against the contaminants. The key contaminants identified on the membrane surface were carbonates and sulfates of calcium and magnesium, so their pre-treatment with electro-coagulation (EC) was targeted. The EC process was systematically optimized for the electrode connection, electrode arrangement, current density, reaction time, and electrode material. Maximum removal observed were Mg 100%, Ca 38%, total hardness 68%, and SO<sub>4</sub><sup>2-</sup> 66% at an applied current of 1000 mA for 30 min using a bipolar series arrangement with Aluminum electrodes. The pre-treated stream produced a 35% higher flux in the FO process compared to the untreated stream. The findings of this study could serve a pivotal role in the scale-up applications of EC and FO for water and resource recovery from non-oily effluents from refineries.



# CHAPTER 1: INTRODUCTION

## 1.1 Background

The expansion of the world population has caused pressure on the need to provide fresh water, increasing the need to safeguard the limited freshwater resources available for the future. At the same time, the demand for exploring the use of treated wastewater for various industrial applications, and for direct potability, seems to be escalating. The petrochemical industry is one of the largest user of water because of processes like distillation, liquid/liquid separation, product washing and cooling (Ashtoukhy et al., 2013). It is also a major source of industrial effluent which is defined by high chemical contents including sulfates, magnesium, calcium, total hardness, and conductivity. If petrochemical wastewater is not adequately treated, it can lead to increased pollution of surface water and ground water through percolation to the water bodies and other water resources which negatively impact the surrounding flora and fauna (Khaing et al., 2010). Some of the prominent pollutants found in petrochemical wastewater are inorganic and organic, which poses severe threats to the environment if not handled in an appropriate way (Clemente et al., 2015). Such contaminants have the potential to accumulate in the environment, thus requiring enhancement of the techniques and effectiveness of treatment and recovery.

The current trend is to design technologies for efficient wastewater treatment and enable efficient extraction of the targeted pollutants. The advanced technologies utilized in the improvement of water recovery include electrocoagulation (EC) and forward osmosis (FO) since the petrochemical industry has adverse effects on the environment. Such technological strategies can indeed improve the sustainability and, in turn, the economy of

the industry in terms of decreasing liquid and hazardous chemical emissions (Li et al., 2020).

## **1.2 Problem Statement**

Most petrochemical industries generate huge amounts of complex wastewater that is very difficult to treat using the conventional treatment processes. It results in environmental pollution and violation of the established legal requirements. Currently, there is a pressing need for improved technology that can deal with non-oily water effluents and treat it efficiently and manage the resources to minimize impacts. Realizing a zero liquid discharge (ZLD) or minimal liquid discharge (MLD) in the petrochemical industry with the help of conventional biological or physico-chemical processes is difficult as such treatments eliminate the contaminants and create hazardous sludge as by-products that are unsafe to release into the environment (Wang et al., 2020). Furthermore, there are contaminants that intervene when broken down by the biodegradation process, and turn into carcinogenic substances. Hence, it is impossible to optimize ZLD without negatively impacting other process streams derived from the same sources, such as the petrochemical sector.

An ideal draw solution for recovery of the contaminant should possess low reverse solute flux and does not require the draw solution regeneration. By implementing FO, with an ideal draw solution, the petrochemical industry can move closer to achieve its steps toward ZLD, recover more water, diminish the sector's negative implications on the environment, and make the industry more sustainable.

### **1.3 Significance and Novelty**

The importance of this study lies in the ability of electro-coagulation and FO to reform the method of wastewater treatment in the petrochemical industry. The use of tetra ethyl ammonium bromide (TEAB) as DS and different electric arrangement of EC setup can be novel in treating petro-chemical non-oily stream. The findings of the research will help to refine the general understanding of the overall efficiency and requirements of EC and FO in different operational conditions, to make a better understanding of how fouling acts on a membrane surface and find out the removal efficiency of the main contaminants. This research focused on the application of EC and surfactant-driven forward osmosis (SDFO) for water reuse in non-oily wastewaters in the petrochemical sector. This includes measuring the level of contaminant rejection by the FO membrane, assessing the membrane's ability to generate flux, and evaluating the reverse solute flux (RSF) of the surfactant TEAB when simulated petrochemical wastewater is used as the feed solution. The impact of factors such as temperature and cross flow velocity, which define the major process parameters, were studied in detail. Major foulants were identified to investigate their behavior as they interacted with the active groups on the membrane active layer in order to mitigate the fouling. Moreover, the study investigated the efficiency of the SDFO process through comparing the results between the process with and without pre-treatment by electrocoagulation to check whether this process helps to evaluate the efficiency of treatment. The present extensive analysis aims to enhance the EC and SDFO systems to help achieve the ZLD goals of the petrochemical sector by increasing the recovery of water and reduction of contaminants.

## **1.4 Research Objectives**

The main objective of the study are as follows:

1. Examine the types of fouling that occur on the membrane surface during the FO process.
2. Develop strategies to mitigate fouling and scaling to maintain membrane performance.
3. Assess the removal efficiencies of sulfates, magnesium, calcium, total hardness, conductivity, under different operational conditions of EC.
4. Compare the flux produced in the FO process with and without pre-treatment using EC to determine the effectiveness of pre-treatment in enhancing the FO process.

## CHAPTER 2: LITERATURE REVIEW

### 2.1 Water Scarcity as a Global Issue

Water scarcity is an increasing global challenge. Despite water covering about 70% of the Earth's surface, only 3% of it is freshwater, and merely a third of that is accessible, with the rest frozen in glaciers and ice caps. Industrial and urban development have continuously reduced freshwater availability. Pakistan has also become water scarce country. From 1996 to 2006, per capita water availability dropped from 1,299 m<sup>3</sup> to 1,100 m<sup>3</sup>, and it is predicted to fall below 700 m<sup>3</sup> by 2025 (Khan et al., 2019). Currently, around 2.1 billion people lack access to safe drinking water (UNICEF, 2019), and projections suggest that by 2050, this number will increase to 4 billion (Orimoloye et al., 2021).

Wastewater reuse and recycling are critical solutions to mitigate water scarcity and meet the increasing demand. However, globally, 80% of wastewater remains untreated and is discharged untreated into the environment (Mark et al., 2015). In Pakistan, only a small proportion of wastewater is treated.

For the petrochemical industry, a major water consumer, addressing water scarcity involves implementing advanced water recovery and treatment technologies. Techniques such as EC and SDFO are being explored for their potential to effectively treat non-oily wastewater streams (Furaiji et al., 2019). By optimizing these methods, industry can reduce its freshwater usage, minimize environmental impacts, and progress towards ZLD goals, thereby ensuring a sustainable water supply for future needs.

## **2.2 Water Consumption in the Petrochemical Sector**

Water is not only essential for life, but it is also used in large amounts in petroleum drilling and refining (Sun et al., 2018). Other than acting as a medium through which reactions occur, water is a crucial factor for various functional specifications that are significant within the system, equipment, and generation of hydrocarbons.

### *2.2.1 Drilling Processes*

Water is important within the petrochemical industry with regards to drilling operations regarding hydrocarbons for instance, oil and natural gas. Its utilization in drilling encompasses several key functions such as:

#### *2.2.1.1 Drilling Fluid Composition*

Drilling fluids or muds are essential in drilling operation. These being a water base product that are used to cool the drill bit, support, and maintain the stability of the well bore opening and lift cuttings from the bottom of the well to the surface. Thus, the heat and pressure of the water-based drilling fluids are essential to the efficiency of drilling and the protection of equipment.

#### *2.2.1.2 Hydraulic Fracturing*

Through the application of hydraulic fracturing, water is pumped at high pressure in order to break the rock and release the hydrocarbons locked inside. This process also helps in increasing the production capabilities of oil and gas and in the transportation of proppants that help maintain the fractures and increase the flow of hydrocarbons (Wei et al., 2018).

### 2.2.1.3 Pressure Control and Formation Stability

Water assists in controlling well bore pressure, avoiding blowout and to obtain stable formation. Since the water can easily adjust to the pressures down the hole, it is appropriate for handling the many and diverse pressures experienced while drilling (Luo et al., 2022).

## 2.2.2 Refining Processes

Water is vital in refining processes, supporting various stages of transforming crude oil into valuable petrochemical products:

### 2.2.2.1 Cooling Systems

Cooling is another function of water, and this is due to heat that is produced when refining is going on and water is used to absorb that heat. It is crucial to optimize heat conditions of the equipment by using water cooling in order to preserve the functionality and prevent issues during the process of refining (Farahani et al., 2016).

### 2.2.2.2 Steam Generation for Distillation

Steam is used in distillation of the crude oil into its fractions, and this is dependent on water as the main medium for steam production. Steam generation makes it possible to heat crude oil to the appropriate temperatures that are useful in separating the hydrocarbons depending on their individual boiling points (Bai et al., 2019).

### 2.2.2.3 Chemical Processing and Reaction Medium

The following refining chemical processes are examples where water is both a solvent and a reacting medium: hydrocracking, hydrotreating and catalytic reforming. The solvents and carriers are significant in hauling reactants and products and are crucial for the chemical transformation and refining effectiveness (Bai et al., 2019).

#### 2.2.2.4 Desalting and Contaminant Removal

The main use of water in desalting is to wash crude oil in order to strip the salts which are detrimental to the refining equipment or to the finished products. This is evident that this application of water is suitable for further processing (Degnan, 2015).

### **2.3 Characteristics of Refinery Petrochemical Wastewater**

Refinery petrochemical wastewater contains a number of pollutants which originate from different petrochemical processes operating within the refinery as shown in **Table 2.1** (Jia et al., 2019; Ye et al., 2020).



**Table 2.1:** Characteristics of real wastewater

<b>Parameters</b>	<b>Units</b>	<b>Real Wastewater</b>
<b>Conductivity</b>	uS /cm	20,182
<b>TDS</b>	ppm	10,470
<b>pH</b>	-	6
<b>Turbidity</b>	NTU	1
<b>COD</b>	ppm	0
<b>Oil &amp; grease</b>	ppm	2.2
<b>TSS</b>	ppm	2
<b>Sodium</b>	ppm	2,575
<b>Potassium</b>	ppm	166
<b>Calcium</b>	ppm	520
<b>Magnesium</b>	ppm	145
<b>Chloride</b>	ppm	5,690
<b>Sulfate</b>	ppm	638

## **2.4 Need for Wastewater Reuse**

Reusing treated wastewater is increasingly important due to several factors:

### *2.4.1 Water Scarcity*

Most areas today, particularly the dry areas, are experiencing a crunch on water supply and demand. Recycling wastewater can complement freshwater and sustain many applications such as industrial, agricultural, and even potable uses.

### *2.4.2 Environmental Protection*

Discharging untreated produced water releases the suspended and dissolved contaminants to the adjacent soil, surface water, and possibly groundwater. Recycling treated wastewater helps reduce pollution and promotes environmental sustainability.

### *2.4.3 Regulatory Requirements*

Strict environmental standards across the world scrutinize industrial wastewater effluent. Such regulations can be a challenge to some industries, which need to meet such guidelines to avoid penalties and compelling them to use treated wastewater.

### *2.4.4 Economic Benefits*

Reuse of treated wastewater decreases the burden of freshwater procurement and wastewater discharge. It also provides reliable supply of water for industrial uses, thus decreasing the supply from external sources.

#### *2.4.5 Resource Recovery*

The treated wastewater is another source of opportunity to recover nutrients, energy, and other valuable products, including, nutrients that can be reused in the agricultural sector and biogas that can be produced out of organic residue.

Based on these considerations, improving effective and inexpensive technologies for treatment of produced water is imperative to enable its recycling and support lasting techniques for water usage.

### **2.5 Existing Treatment Methods**

To cater the problem of petrochemical wastewater, several treatment techniques have been formulated and deployed physically, chemically, biologically, and the advanced state of the art membrane processes (Santos et al., 2020). This is because each technique has its benefits and drawbacks. This means that in most treatment procedures, two or more techniques are used in order to come up with a treatment plan that serves the intended purpose.

#### *2.5.1 Physical Treatment Methods*

##### **2.5.1.1 Gravity Separation**

Coalescing floaters, Corrugated Plate Interceptor separators, dissolved air flotation (DAF), etc. are some of the common treatment techniques that help in eliminating oil and suspended solids in petrochemical wastewater by following the density principle.

##### **2.5.1.2 API Separators**

These systems enable oil to form a layer on top of water because it is lighter while the sediments sink to the bottom as a result of gravitational force. One study shows that large droplets of oil and suspended solids in refinery wastewater can be effectively separated by API separators (Saththasivam et al., 2016). On the other hand, their efficiency reduces for the small sizes of the emulsified oil droplet and fine particulate matters.

#### 2.5.1.3 Dissolved Air Flotation (DAF)

DAF systems add air bubbles to the wastewater and these bubbles fix themselves on oil droplets as well as suspended solids that float on water surface. According to the studies, DAF is capable of removing fine droplets of oil and even particles with small sizes owing to its high efficiency of emulsified oils as well as colloidal matter removal.

#### 2.5.1.4 Filtration

Some of the methods of petrochemical wastewater treatment include sand filters, multimedia filters and cartridge filters for filtering out the suspended solids and colloids. These types of filters use sand or other granular filters to affect the removal of suspended particles and colloidal matter. In one study, researchers found that multimedia filters significantly reduce turbidity and particulate matter; however, they clog quickly and require frequent backwashing.

#### 2.5.1.5 Cartridge Filters

Cartridge filter applies the use of replaceable cartridge to trap suspended solids. One study shows that cartridge filters offered a better filtration standard compared to sand filters as they help in polishing the effluent coming from the primary treatment sequence.

#### 2.5.1.6 Centrifugation

In centrifuges, there is a force known as centrifugal force, with the help of which, the oil, solids, and water get separated. Since centripetal force is very weak, the effect of force is to make the heavy particles such as oils to be thrown outwards away from the lighter water particles. In the study by Tang et al. (2015), it was established that the centrifugation process is effective in the removal of fine particles and emulsified oil, but the process is energy intensive with high operation costs.

#### 2.5.2 *Chemical Treatment Methods*

##### 2.5.2.1 Coagulation and Flocculation

Other chemicals include chemical coagulants like aluminium sulfate (alum) and ferric chloride that work by destabilizing colloidal particles and forming flocs. Coagulants overcome the charges on colloidal particles hence facilitating aggregation of the particles into larger particles.

##### 2.5.2.2 Oxidation

Chlorine, ozone and hydrogen peroxide oxidize organic pollutants and disinfect wastewater. Chlorine and ozone are oxidizing agents that cleave organic compounds and also kills pathogens. This is because oxidizing agents cause the oxidation of organic molecules. Also, Wang et al. (2016) reported that the use of ozone causes elimination of color, odour and of persistent organic pollutants in petrochemical wastewater (Gagol et al., 2018). But one disadvantage of chlorination is that it forms potential trihalomethanes (THMs), which are unhealthy for consumption.

### 2.5.2.3 pH Adjustment

By altering the pH of the petrochemical wastewater, it can form flocs which will help in the addition of contaminants through precipitation. Some contaminants can also be precipitated depending on the pH value with respect to water treatment, for instance, heavy metal ions.

## 2.5.3 *Advanced Treatment Methods*

### 2.5.3.1 Membrane Filtration

Micro filtration (MF), ultra-filtration (UF), nano filtration (NF), and reverse osmosis (RO) technologies all employ a membrane-based separation technique, which separates contaminants on the basis of their size or on their charged status.

### 2.5.3.2 Microfiltration and Ultrafiltration

These membranes filter out and repel dispersed phases, bacteria, and large organic molecules. UF helps in polishing effluent from biological treatment processes. UF is highly susceptible to fouling (Padaki et al., 2015).

### 2.5.3.3 Nanofiltration and Reverse Osmosis

NF and RO give further purification by the removal of dissolved salts, small organic molecules, heavy metals for instance. In the study conducted by Zhou et al. (2015), it was observed that RO has a high level of efficiency in desalination but works under high pressure and acts vulnerable to sealant deposits and fouling.

#### 2.5.3.4 Membrane Distillation (MD)

MD is a thermal-driven process; the transfer of water vapor across a hydrophobic membrane occurs from the hot feed phase to a cold permeate phase. Because of the presence of heat, there is a variation in vapor pressure, and water vapor passes through the membrane escorting the contaminants. MD is most appropriate for treating the high-salinity wastewater though it can have scaling issues (Lloyd, 1997; Veleva et al., 2021).

### 2.6 Forward Osmosis (FO)

In FO the water diffusion process is influenced by the osmotic pressure of feed and draw solutions, and it is based on selective permeability of a semi-permeable membrane.

#### 2.6.1 Operation

The feed solution that has lower osmotic pressure is constantly fed to the membrane that draws water from solution due to higher osmotic pressure of draw solution. The contaminants stay in the feed solution, while permeates moves to draw solution. McCutcheon et al. (2006) in his study clarified that FO works at a relatively lower pressures than RO hence suitable for petrochemical wastewater.

#### 2.6.2 Mechanism of FO

##### 2.6.2.1 Osmotic Pressure Difference

In terms of mechanism of action, FO utilizes osmotic pressure difference between two solutions. The feed solution, such as petrochemical wastewater, has low osmotic pressure, while the draw solution, like concentrated brine, exhibits significantly higher osmotic

pressure (Nawaz et al., 2021). This process occurs as a result of the diffusion of water due to the natural osmotic pressure difference prevailing from the feed solution to the draw solution through the semi permeable membrane. Contaminants are stuck on the feed side of the membrane.

#### 2.6.2.2 Membrane Structure

FO membranes are thin-film composite membranes consisting of a thin film selective layer overlaid on a support layer (Ifakhar et al., 2020). The selective layer is made to allow water molecules to pass through but to exclude salts or other impurities. Support layer offers structural support and tackles experience of internal concentration polarization that is known to lower the water permeation.

#### 2.6.2.3 Draw Solution Regeneration

This diluted draw solution requires regeneration to restore the osmotic pressure gradient that permits the accumulation of the solutes of interest. This can be made possible by passing the dissolved substances through processes like MD, RO, or thermal desalination (Nawi et al., 2020).

#### 2.6.3 *Use of TEAB in petro-chemical industry*

TEAB is used commonly in petrochemical industry because of the following reasons: thermal stability, solubility in water and more importantly it acts as a structure directing agent (SDA). Such characteristics make TEAB especially suitable to be used in several petrochemical processes. For example, in the production of lubricants and diesel fuels, TEAB is employed in that it promotes the creation of large molecular structures that



improve on the performance and stability of the end products. This is important to obtain the right viscosity and thermal stability of high-performance lubricants and diesel fuels as mentioned (Yoo et al., 2003).

Moreover, TEAB is extremely involved in the cracking of olefins for creation of propylene as one of the most elementary commodities essential in the construction of various petrochemical commodities. In essence, as an SDA, TEAB helps in the cracking process, and in the creation of the right molecular structures needed during the catalytic process. This is important for breaking down much larger molecules of hydrocarbons into smaller and more useful molecules such as propylene. Another work investigates the interaction of air bubbles with the air-water interface and shows that TEAB affects surface tension and bubble stability; this factor is vital in the gas-liquid separation as well as interactions with gas bubbles (Ghosh, 2004). TEAB is used in the separation of benzene and cyclohexane by the process of extractive distillation. This research proves that TEAB is useful when it comes to increasing the separation efficiency which benefits the purity as well as yield of petrochemical products (Wang et al., 2022).

TEAB could maybe be reused in other processes in the refinery depending on the specifications of the application. On the other hand, if the concentration is higher than the concentration required in the other processes, it may be diluted to the concentration that is ideal for efficient use. Aqueous solution of tetraethyl ammonium bromide (TEAB) is used to prepare advanced catalysts for ultra deep hydro desulfurization (HDS) in the petroleum refinery. It is also used as a hybrid agent for preparation of tungsten (W) and molybdenum (Mo) precursors for the synthesis of a trimetallic WMoNi-Al<sub>2</sub>O<sub>3</sub> catalyst. For enhancing the textural and chemical synergisms in the catalyst, TEAB helps in synthesizing the hybrid

organic-inorganic nano crystals required for their development. These TEAB-stabilized HNCs are then used to synthesized oxidic  $W\text{MoNi-Al}_2\text{O}_3$  into which is impregnated nickle nitrate ( $\text{Ni}(\text{NO}_3)_2$ ). The new trimetallic catalyst thus increases efficiency in sulfur removal within diesel fuels, enhancing HDS performance (Shan et al., 2016). Tetraethylammonium bromide is a favorable kinetic inhibitor against gas hydrate formation in pipelines of oil and gas industries at the concentration of 0.05 to 0.1 mf. TEAB effectively delays the rate of nucleation of methane hydrates by about 141% (19.5 hours) as compared to the pure methane hydrate and therefore can be used for flow assurance. This assists to prevent the formation of blockages that may hinder the flow of oil and gas through offshore pipelines. The application of TEAB in the refining processes yields a more efficient and steady supply of hydrocarbons with the high pressure and low temperature processes (Gupta et al., 2022). TEAB can withstand high temperatures during the crystallization of zeolite without decomposing.

#### *2.6.4 Advantages of FO*

One of the major advantage of using FO is that pressure difference is low, consequently, membrane is not forged and will last longer, meaning less expenses in replacement. For high osmotic pressure wastewater like high salinity, FO is preferable given the fact that different FO membranes can maintain their flux rates while being challenged with high osmotic pressures (Nawaz et al., 2022).

#### *2.6.5 Challenges of FO*

##### *2.6.5.1 Draw Solution Management*

It is crucial to select and manage the draw solution to maintain the efficiency of FO process (Shaffer et al., 2015).

#### 2.6.5.2 Internal Concentration Polarization (ICP)

The desired site of ICP is thus in the plane of the support layer in the composite membrane and because of this the effective osmotic pressure differential as well as water permeability is decreased (Cath et al., 2006). It remains clear that in order to reduce ICP, more attention should be paid not only to the choice of membranes, but to the physical arrangement of the modules as well.

#### 2.6.5.3 Limited Commercial Availability

In retaining an academic focus, FO is still considered as a relatively novel technology with minimal industrial applications at a commercial scale. The improvement of membrane materials and the designs of the systems, on its other part, still require more advancements in knowledge in the future.

#### 2.6.5.4 Membrane fouling

One major concern in operating membrane treatment systems is the fouling of the membrane surface. Some of these causes include the presence of various inorganic compounds and colloidal particles combined with dissolved matter and microorganisms in the feed solution (Nawaz et al., 2024; Yasmeen et al., 2023). Such contaminants can either deposit on the membrane surface or even get entrapped in the pores of the membrane, thus creating a decline in the performance of the membrane, and also increases the need for

cleaning to enhance performance, thus increasing the operational costs (Alamoudi et al., 2022; Sahebi et al., 2020).

## 2.6.6 *Key Factors Contributing to Fouling in FO*

### 2.6.6.1 Low Water Flux

FO is less sensitive to feed water flow rate when compared with RO, which indicates that lower transport rate of contaminants exists in the FO system and these contaminants are deposited to a lesser extent on the membrane surface.

### 2.6.6.2 Membrane Characteristics

The smoothness of the membranes used in FO and their affinity for water also helps to reduce fouling to an appreciable level. Fouling is normally caused by the accumulation of organic and biological materials on the surfaces of a material and therefore surfaces with a high affinity for water are least likely to be fouled.

### 2.6.6.3 Hydraulic Pressure

FO works at or very near the atmospheric pressure which means that there is very little hydraulic pressure that causes fouling of foulants to stick much on the surface of a membrane. This is different for RO as higher pressure has significant negative effects of fouling.

### 2.6.6.4 Cross Flow Velocity

The extent of crossflow velocity has a proven optimal way of reducing organic fouling through its continuous sweeping action of foulants from the fiber membranes of FO

(Yasmeen et al., 2023). This flow keeps stirring the system so as to hinder fouling layer build up.

#### 2.6.6.5 Organic Fouling Control

In other words, since petrochemical wastewater tends to have high concentrations of organic loading, fouling has to be adequately addressed. According to Lay et al. (2010), a benefit that FO offers over RO is fouling control, that is, the ability to control the fouling rate through crossflow velocity.

### 2.7 Electrocoagulation (EC)

EC also incorporates sacrificial electrodes to produce coagulant species locally, and thus destabilize and coil up the contaminants to enable their elimination.

#### 2.7.1 Operation

In electro-coagulation, an electric current causes the metal electrodes to dissolve while releasing coagulant species (e.g., iron or aluminium hydroxides) into the water. These coagulants are used for charging elimination on defined colloidal particles by forming flocs that can easily undergo sedimentation or filtration. According to research conducted, it was revealed that EC can effectively remove colloidal particles, heavy metal ions, and organic pollutants and therefore could be used as a pre-treatment option for membrane solution systems (Davarnejad et al., 2014).

#### 2.7.2 Mechanism of EC

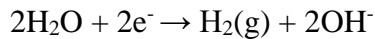
##### 2.7.2.1 Electrode Reactions

At the anode (positive electrode), the metal dissolves to form metal cations such as  $\text{Al}^{+3}$  or  $\text{Fe}^{+2}/\text{Fe}^{+3}$ . These cations react with hydroxyl ions ( $\text{OH}^-$ ) in the water to form metal hydroxides.

For Aluminium:  $\text{Al} \rightarrow \text{Al}^{+3} + 3\text{e}^-$

For iron:  $\text{Fe} \rightarrow \text{Fe}^{+2} + 2\text{e}^-$  (can further oxidize to  $\text{Fe}^{+3}$ )

At the cathode (negative electrode), water is reduced to produce hydrogen gas and hydroxyl ions.



#### 2.7.2.2 Coagulation and Flocculation

The metal hydroxides formed in situ act as coagulants. These hydroxides neutralize the charges on colloidal particles, causing them to aggregate into larger particles (flocs). This process is known as coagulation (Abbar et al., 2021). The flocs formed during coagulation can capture and bind with various contaminants, including suspended solids, heavy metals, and organic pollutants.

#### 2.7.2.3 Separation

The larger flocs can then be separated from the treated water by sedimentation, flotation, or filtration. The hydrogen gas produced at the cathode helps in the flotation of the flocs, enhancing their removal.

### 2.7.3 *Operational Parameters Affecting EC*

#### 2.7.3.1 Current Density

It is the amount of electric current applied per unit area of the electrode surface. Higher current densities can increase the rate of metal dissolution and coagulant production, but they also raise energy consumption and cause electrode wear (Giwa et al., 2012; Yan et al., 2011).

#### 2.7.3.2 Electrolysis Time

The duration for which the electric current is applied is a crucial factor for removal of impurities. Longer electrolysis times can enhance contaminant removal but also increase energy consumption (Hamada et al., 2018; Khalifa et al., 2022; Yavuz et al., 2010).

#### 2.7.3.3 pH

The pH of the wastewater influences the solubility of metal hydroxides and the efficiency of coagulation. Generally, a neutral to slightly alkaline pH is optimal for the formation of metal hydroxides (Pérez et al., 2016; Sardari et al., 2018; Yan et al., 2014).

#### 2.7.3.4 Inter-Electrode Distance

The distance between the anode and cathode affects the efficiency of the process. A shorter distance reduces electrical resistance and energy consumption (Moussavi et al., 2011).

### 2.7.3.5 Electrical Arrangements of electrodes

Electrodes placement is crucial in EC systems as the design affects the system's performance and efficiency. There are primarily three electrical connections for different arrangements; they are, Mono-Polar Series (MP-S), Mono-Polar Parallel (MP-P), and the Bi-Polar Series (BP-S), each having their different effects on voltage and current as shown in **Figure 2.1**. In the case of the Mono-Polar Series configuration, the electrodes of the pair are connected in series; the total voltage thus sums up the voltage across each pair of electrodes, but the current remains the same. This setup is preferred in situations where there is the need for a high voltage and a low current flow, mostly in situations whereby the distance between the electrodes can be controlled to reduce the high resistance problem. In the case of the Mono-Polar Parallel connection, all the electrode pairs are linked in parallel. Here the voltage across each electrode pair is the same but the current varies in all of the electrode pairs. Due to the uniform distribution of current over several electrodes, this configuration is suitable for structures with low voltage and high current, which is suitable for large treatment structures. The last configuration in the Bi-Polar Series configuration is where only the outermost rods are connected to the power supply while inside rods act as both anode and cathode. Furthermore, it permits the total voltage to build up in the electrode while it possesses constant current. The bi-polar series is characterized by energy efficiency and less wiring else because of its structure, which may mean that it will be easier to maintain and therefore cheaper to operate (Jasim et al., 2023).



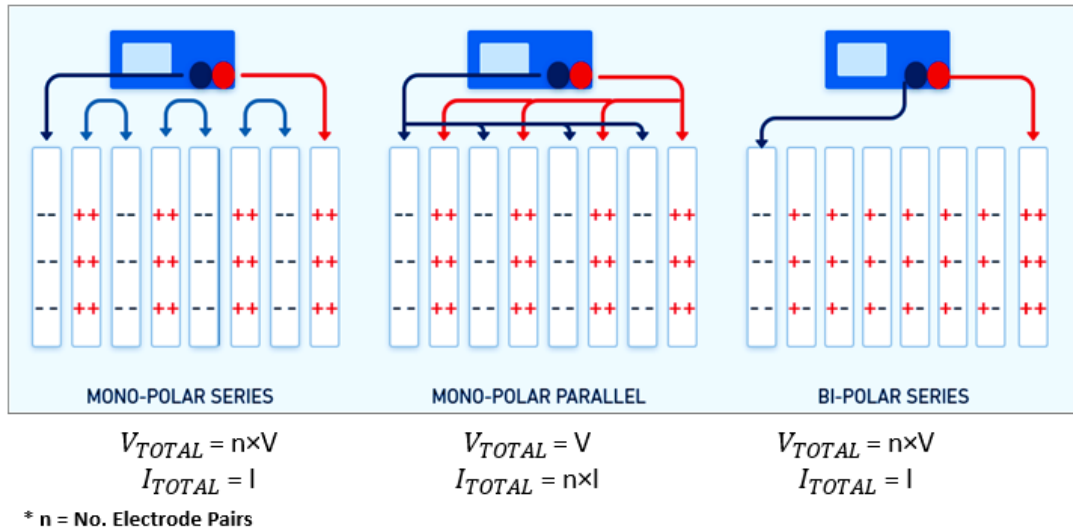


**Figure 2.1:** Electric arrangement in electro-coagulation

#### 2.7.4 Advantages of EC

**Effectiveness:** EC can effectively remove a wide range of contaminants, including suspended solids, heavy metals, and organic pollutants (Nawaz et al., 2024).

**Simplicity:** The process is relatively simple and does not require the addition of chemical coagulants, reducing the need for chemical handling and storage.

**Sludge Characteristics:** The sludge produced by EC is generally easier to dewater and handle compared to sludge from chemical coagulation.

#### 2.7.5 Challenges of EC

**Energy Consumption:** The process can be energy-intensive, especially at high current densities and long electrolysis times.

Electrode Consumption: The sacrificial electrodes are consumed during the process and need to be replaced periodically, adding to the operational cost (Akkaya, 2022).

Scalability: While EC is effective at small to medium scales, scaling up the process can present technical and economic challenges.

## CHAPTER 3:     METHODOLGY

### 3.1   Characterization of synthetic wastewater

To test the effectiveness of two technologies EC and FO on effluent of petrochemical industry, a synthetic wastewater recipe is developed as described in **Table 3.1**. This synthetic wastewater mimics the properties of real petrochemical wastewater in order to acquire conditions that are manageable and feasible within the experiments. The real wastewater samples were taken from a local refinery in Pakistan. The **Figure 3.1** shows the key scheme of wastewater generation in local petro-chemical refinery. To synthesize the wastewater in the lab, deionized water was employed in the process to remove any interference from impurities. The salts were dissolved in deionized water to get the required concentrations of the salts. The glucose was added to represent the COD concentration, while the colloidal silica was predominantly used to determine the level of turbidity and TSS (Nawaz et al., 2021a). The maximum oil and grease concentration in a real wastewater sample was 2.17 mg/L. As for evaluation in the worst-case scenario, the concentration of 10 mg/L was added. The oil used in the experiments was the standard emulsion of oil in water droplets, consolidating the existence of the most immense challenges that may be encountered. Also, humic acid (HA) was introduced as a model foulant for natural organic matter in this work (Nawaz et al., 2021b). The synthetic wastewater was then analyzed using some standard parameters in order to confirm its authenticity with real petrochemical effluents.

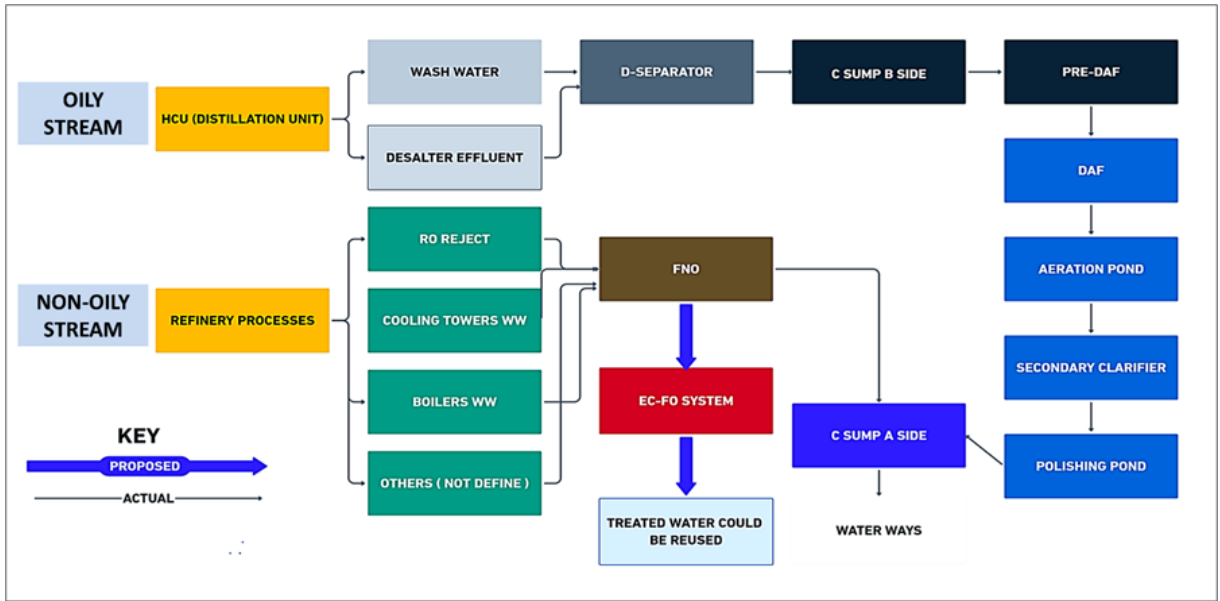


**Figure 3.1:** Wastewater Generation Scheme

**Table 3.1:** Composition of synthetic final non-oily stream

<b>Synthetic Wastewater Recipe (mg/L)</b>		
	<b>Final Non-Oily Stream</b>	
<b>NaCl</b>	5,767	Diesel = 10 mg/L Glucose = 100 mg/L Humic acid = 20 mg/L
<b>KCl</b>	316	
<b>CaCl<sub>2</sub></b>	2,602	
<b>MgCl<sub>2</sub></b>	570	
<b>Na<sub>2</sub>SO<sub>4</sub></b>	942	
<b>BaCl<sub>2</sub></b>	2	
<b>SrCl<sub>2</sub></b>	70.5	
<b>Silica</b>	19.6	
<b>TDS</b>	10,291	

### 3.2 Draw Solution

In this research, the surfactant TEAB was used as the DS since it has the ability to maintain a constant osmotic pressure and also has lower reverse solute flux (RSF). The TEAB employed in this study was of a laboratory grade and was purchased from the Sigma-Aldrich Company based in the United Kingdom.

### 3.2.1 TEAB

TEAB is quaternary ammonium compound with the formula  $C_8H_{20}N^+Br^-$  and has molar mass of 210.16 g/mol. This product is soluble in water and has been determined to have a critical micelle concentration of 0.16 mol/L and density of 1.4 g/cm<sup>3</sup>. TEAB is used in FO due to its cationic charge, because it can produce a high flux for the application (Yasmeen et al., 2023).

### 3.2.2 Properties

#### 3.2.2.1 Solubility and Critical Micelle Concentration (CMC)

TEAB is readily soluble in water. The critical micelle concentration of TEAB is the concentration at which it begins to self-assemble into micelles in aqueous solution. This value is generally obtained through experimentation and is assumed to be sensitive to the temperature, ionic strength, and other solutes.

## 3.3 Description of Experimental Setup

### 3.3.1 Membrane Specifications

In all experiments, polyamide-TFC flat sheet FO membranes were used, purchased from Toray Chemicals, Korea. The membrane has a coefficient of water permeability of 6.4 (L/m<sup>2</sup>/h) LMH/bar. The structural parameter of the support layer is 409 μm. Membranes were stored at a laboratory temperature of 24 ± 1°C in DI water, which was replaced weekly. Both batch and semi-continuous experiments were performed to assess the system efficiency. The membranes used were stored at laboratory temperature of 25±1°C in

ultrapure DI water, and the water was changed on a weekly basis to eliminate biofilm formation and for the membranes to function efficiently. Active layer facing feed solution in all the experimental configurations was employed.

### **3.4 FO Batch Study**

This research incorporated both batch and semi-continuous setups. The FO batch setup is described in **Figure 3.2**. The setup includes two variable-speed peristaltic pumps (BT300–2J, Longer Pump, China), a standard acrylic membrane cell featuring two symmetric channels (dimensions:  $10.5 \times 4 \times 0.1$  cm), a weighing balance (UX6200H, Shimadzu, Japan), a temperature controller (TPM-900, Sanhng, China), a hot plate (PC-420D, Corning, USA) and two electrical conductivity meters for the feed and draw solutions (HI2003 edge, HANNA Instruments, USA).

The feed solution and draw solution tanks, with 1L capacity each, were connected with the closed-loop channels in a counter-current flow direction. The duration of batch experiments was 20 hr, and semi-continuous was 48 hr. The active layer facing feed solution (AL-FS) configuration was used in all experiments, and crossflow velocity (CFV) and temperature of the feed side were changed systematically and optimized for semi-continuous experiments in the next phase. In each test, a new membrane coupon of an effective area of  $42 \text{ cm}^2$  was cut out from the same membrane sheet. Water flux and RSF were recorded every minute.

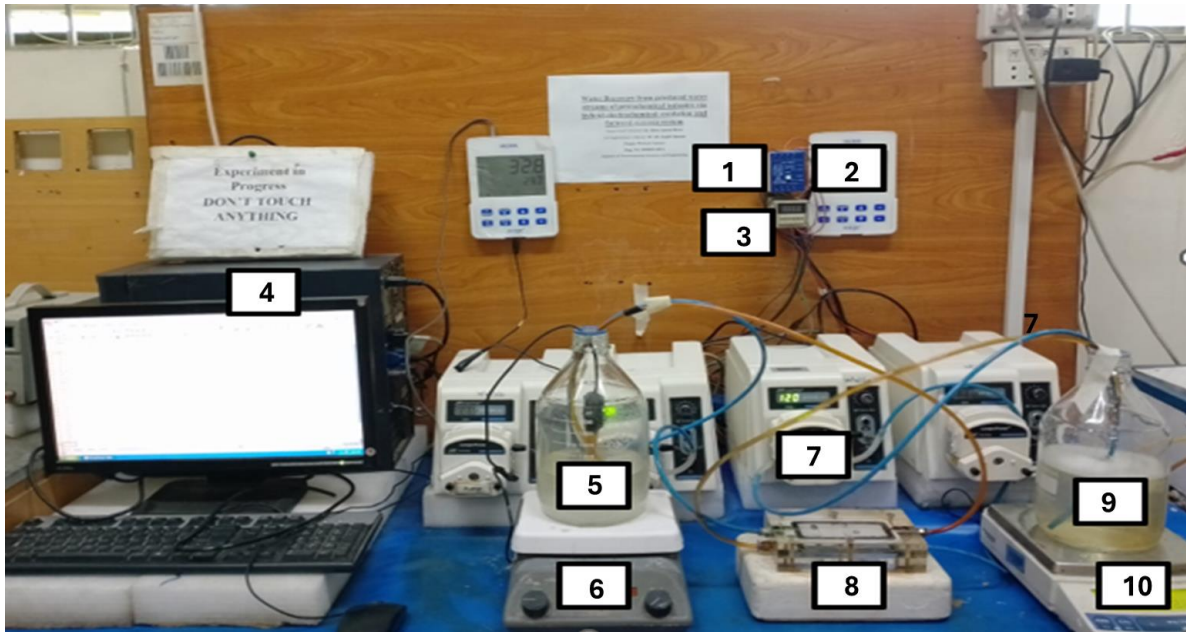


**Figure 3.2:** FO batch setup (1) Level sensor (2) Hanna EC Meter (3) Temperature sensor (4) Data logger (5) Feed solution (6) Hot plate stirrer (7) Peristaltic pump (8) Membrane module (9) Draw solution (10) Weighing balance

### 3.5 EC Batch Study

EC system was used in the batch tests to determine the effectiveness of impurities removal as shown in

**Figure 3.3.** The two particular types of electrodes preferred for this specific application are aluminium and stainless steel. The different current levels were applied to determine the effect of current in the removal of the impurities such as sulfates, calcium, magnesium, and Total Hardness. Each experiment was set for 60 minutes and from the EC chamber, samples were taken at 10 minutes interval to determine the sulfate level as shown in



**Figure 3.4.** The experiments of higher sulfate removal were replicated to study the effects of calcium, magnesium, and total hardness removal. This approach was helpful in identifying the effectiveness of the EC process and the various electrode materials and current levels.

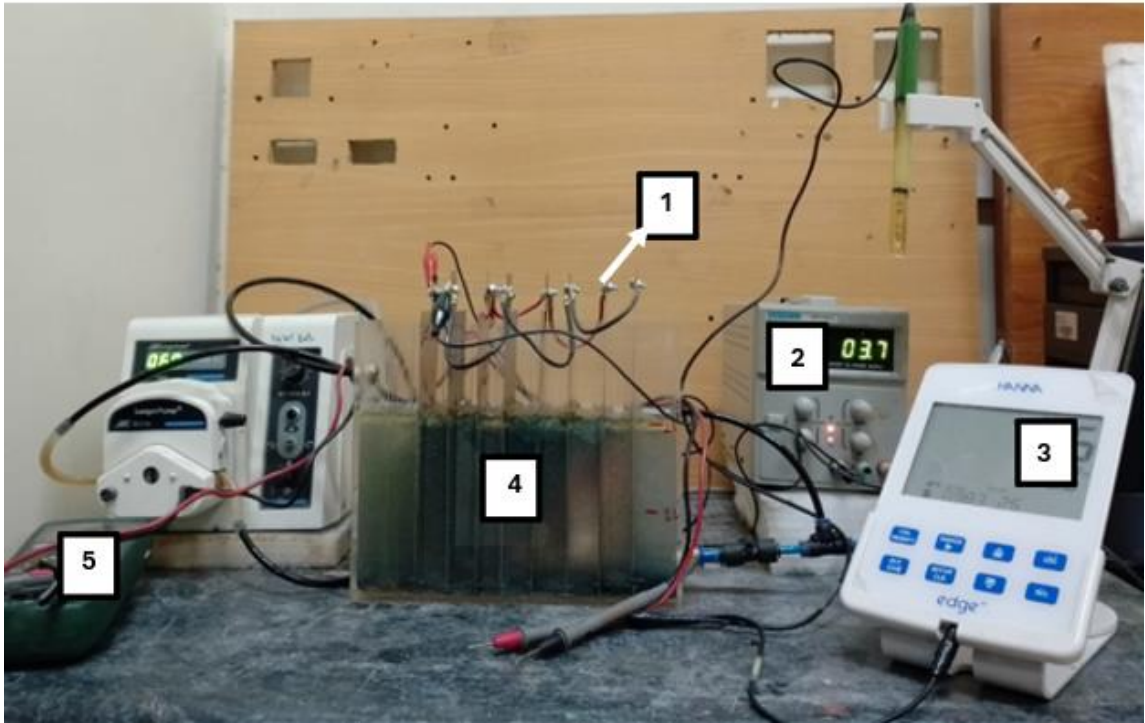


**Figure 3.3:** EC Batch Setup (1) Electrodes (2) DC supply (3) HANNA EC Meter (4) EC chamber (5) pH meter



**Figure 3.4:** Electro-coagulation samples stored for analysis

### 3.6 EC-FO Semi-Continuous Study

According to the optimum results obtained from the batch experiments, a semi-continuous system including EC and FO was applied for 48 hours. In this configuration, wastewater was first treated by using optimized conditions of EC, the permeate of which was the feed solution for FO systems. After the EC process was complete, the FNO stream was shifted to a separatory funnel for 1 hr for the settling of suspended particles. Then, the remaining sludge was separated from the treated FNO stream using a filtration assembly with filter paper ( $0.22\ \mu\text{m}$ ). Before wastewater undergoes through filtration, the wastewater is first allowed to settle in sedimentation assembly. This process helps remove a significant portion of flocs to be removed which reduces the possibility of filter paper to get choked easily. At the beginning of the experiment the volumes of both FS and DS were kept to 1 liter. To maintain the DS surfactant concentration to 0.75 M, a concentrated DS solution

with 4 M TEAB concentration was introduced at a constant flow rate of 1 mL/min with the help of a timer (DH48S, Omron, China). Furthermore, when the FS volume was reduced to 500 mL, DI water was added, and the level was controlled by a level sensor. This schematic diagram of the semi-continuous setup is presented in **Figure 3.5**.

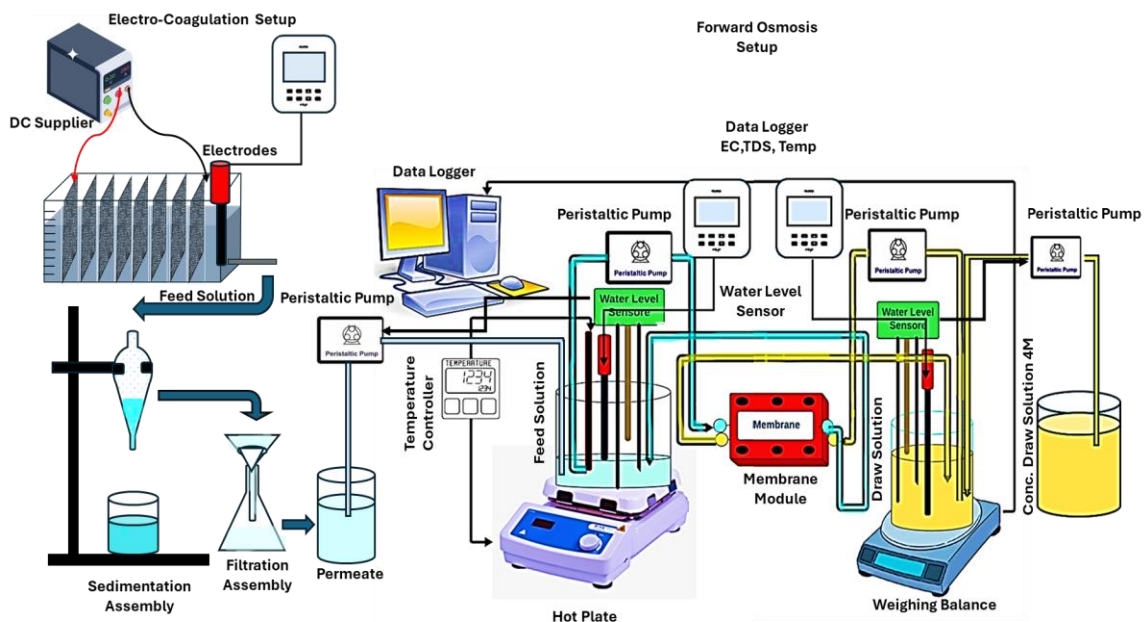


**Figure 3.5:** Schematic Diagram of Electro-Coagulation and Forward Osmosis

### 3.7 Analytical Methods

#### 3.7.1 Calculation of Water Flux and Reverse Solute Flux

The rate of the water transport across the selective layer of the membrane was determined from the changes in the volume of the DS every one minute. To predict the reverse solute flux, conductivity of the FS and DS was recorded every 1 min. The recorded conductivity values were divided by the total volume of FS and DS at the end of the experiment. The amount of salt transfer was calculated as the difference between the initial values of

conductivity and the corrected values based on the specific conductivity coefficient (Nawaz et al., 2021).

### *3.7.2 Analysis of Sulfates, Calcium, Magnesium, Total Hardness, and pH*

The determinations of the samples were made with the following methods of analysis: concentration of sulfate, calcium, magnesium, total hardness, and pH. Sulfates were determined using the turbidimetric method by reacting the sample with barium chloride to form barium sulfate that in-turn forms a turbid solution when precipitated with sample and was quantified with a spectrophotometer (Specord 200 Plus) set at 420 nm. Calcium and magnesium concentrations were determined by atomic absorption spectrophotometry and gravimetrically. In titration method, the one used was EDTA titration which was carried out with a buffer solution at the higher pH of about 10 and an indicator like Eriochrome Black T which reacts with calcium and magnesium ions. Total hardness, as the total concentration of calcium and magnesium ions, was also determined by the EDTA titrimetric method. The pH of the samples was measured with a calibrated digital pH meter, which was calibrated using standard buffer solutions of pH 4, 7, and 10 before and after each measurement the pH meter was rinsed with distilled water. It is evident that these analytical methods offered accurate and reproducible quantification of factors affecting the EC and FO treatments.

## **3.8 Membrane Characterization**

Characterization of the membranes is critical as it can reveal properties of the fouling layer built upon the membrane surface hence it helps to establish efficient control measures. Further, it confirms the orientational order and cross-sectional properties of the membrane

after cleaning (Alamoudi et al., 2022; Veleva et al., 2021). After the experiment, used membranes of each run were dried and stored for analysis. Each membrane sample was cut into two portions; one portion was rinsed with DI water to remove easily detachable contaminants from the membrane sample, while the second portion was not rinsed. Both parts were then slowly air-dried and stored for further characterization phases. This approach guarantees a comprehensive analysis of the impact of on the surface of the membranes.

### *3.8.1 SEM-EDX Analysis*

Due to its ability to provide details of topographical features of the fouling layer as well as the chemical composition, SEM-EDX analysis on AL was performed. In samples preparation for SEM analysis, the samples were placed on conductive adhesive tape and made to adhere on stubs before being coated with a layer of gold or carbon for better imaging. SEM micrographs gathered with high magnification offered clear descriptive information on the membrane fabric surface topographic and fouling profile. Simultaneously, EDX analysis was done to determine the presence and concentration of elements using data gathered from the emitted X-rays upon irradiation of the sample by electron beam. This integration of both SEM and EDX analysis provided a comprehensive information, including the characteristics and composition of the fouling layer, which contributes to the further understanding of strategies to prevent fouling and achieve enhanced membrane performance.

### *3.8.2 Fourier Transform Infrared (FTIR) Analysis*

Surface characterization of the formed fouling layer on membrane surfaces was done through FTIR spectroscopy to identify the chemical functional groups present on the active layer of membrane. Following each experiment, rinsed membrane samples with deionized (DI) water were used to determine the ionic peaks of AL. The dried samples were then characterized using an FTIR spectrometer which scans from around 4000  $\text{cm}^{-1}$  and 400  $\text{cm}^{-1}$  or to determine the various functional groups present. These included respective spectra that exhibited unique absorption bands confirmative of some of the bond types in the fouling materials.

### *3.8.3 Membrane Cleaning*

All the membrane coupons were used for two runs. After the first run of the process, the membrane went through chemical cleaning. Up to 77% water flux could be recovered by chemically cleaning through 0.5% NaOH solution and 2% Citric acid for 10 mins, whereas 55% flux could be recovered by physically cleaning by osmotic backwashing through DI water for 15 mins (Wang et al., 2015).

## CHAPTER 4: RESULTS AND DISCUSSIONS

### 4.1 Effect of Cross Flow Velocity and Temperature

To validate the experimental concept, the CFV and temperature for solution, FS and DS were varied systematically. **Figure 4.1** represents the average hourly flux against different CFVs. The reduction of osmotic pressure is attributed to the dilution of DS (Arcanjo et al., 2020). The highest flux was obtained at a CFV of 8 cm/s, though lower flux rates were recorded at a CFV of 16 cm/s and 24 cm/s. The first part of the increasing trend up to certain levels of CFV can be explained by the decrease in ECP on the AL caused by the scouring effect (Ryu et al., 2020). However, at a very high CFV of 24 cm/s, the feed stream has less time to diffuse through the membrane, and the higher shear forces can lead to pore blocking by breaking down FS particles (Zhang et al., 2021; Nawaz et al., 2019). Hence the overall flux for the given value of CFV 24 cm/s was lesser than that for a CFV of 8 cm/s.

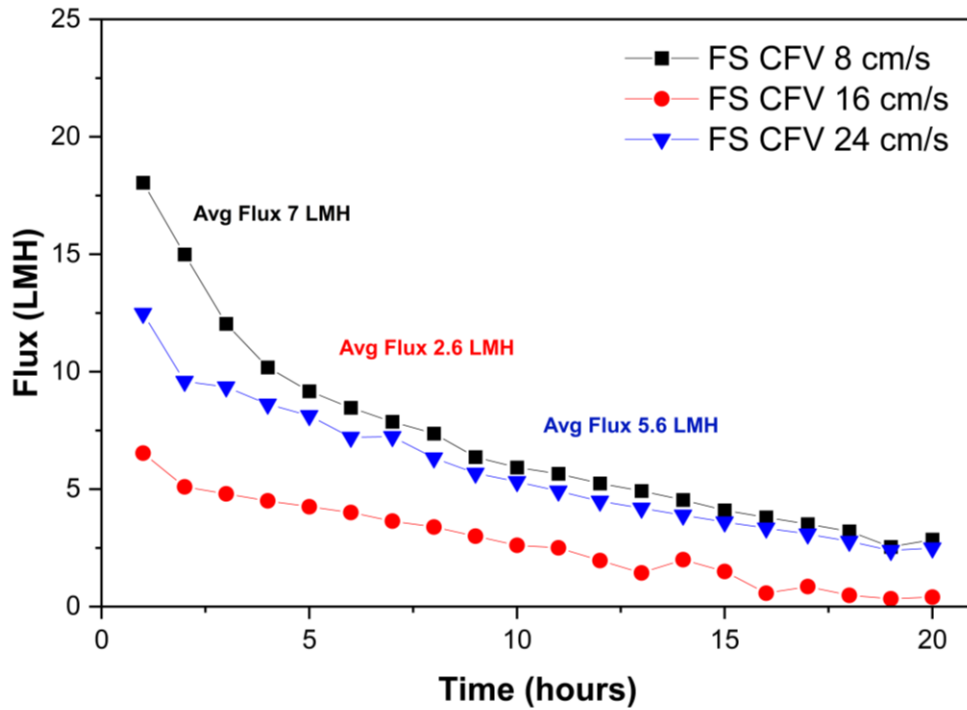


**Figure 4.1:** Flux at different Cross Flow Velocities at 30°C

After the optimization of the CFV, the temperatures of the FS were varied. The temperature of the FS stream was changed from 30°C to 50°C because normally the effluent temperature in the refinery ranges between 30°C and 60°C at the time of generation (Epolito et al., 2008). The values of cumulative gain of conductivities for the FS and DS is shown in **Table 4.1**. It shows that 8 cm/s gave higher flux and lower reverse solute flux (RSF) value. So, lower RSF value of 0.19 GMH suggests 8 cm/s as optimized CFV.



**Table 4.1:** Summary of 20 hrs batch experiments to assess the system performance

<b>Estimation of Average Fluxes and Conductivity Transfer</b>			
<b>FO experiments with different CFV (cm/s)</b>			
<b>Cross Flow Velocities (cm/s)</b>	8	16	24
<b>Average flux (LMH)</b>	7.04	2.56	5.76
<b>Cumulative volume extracted in 20 hrs (mL)</b>	670	244	547
<b>Cumulative gain in conductivity of FS in 20 hrs (mS/cm)</b>	5,357	7,381	16,122
<b>RSF (GMH)</b>	0.19	0.26	0.57
<b>Cumulative gain in conductivity of DS in 20 hrs (mS/cm)</b>	8,029	13,144.5	12,164.5

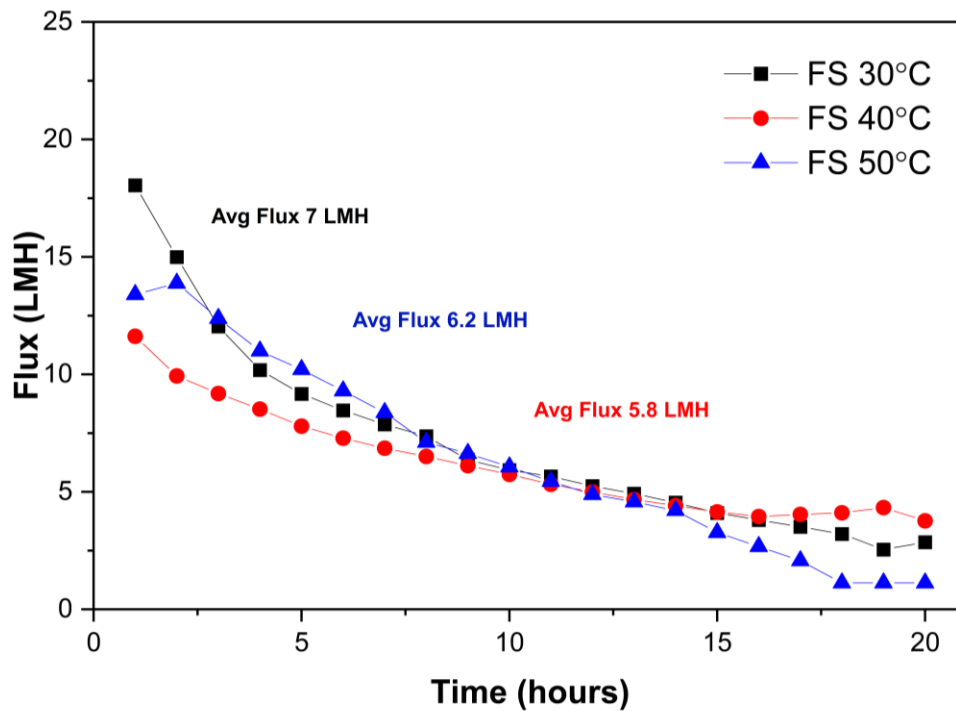


**Figure 4.2:** Flux at different FS temperature at 8 cm/sec cross flow velocity

This is evident from **Figure 4.2** as at an operating condition of FS temperature of 30°C, the highest average flux at 7 LMH is achieved. With the FS temperature at 40°C the average flux was slightly low, being at 5.8 LMH. The average flux increased to 6.2 LMH, when the temperature of the FS was raised to 50°C. Higher flux is seen at 30°C due to the higher osmotic pressure gradient through which water is transported across the membrane. An increase in temperature is accompanied by a decrease in the osmotic pressure gradient and as a result a decrease in flux is observed. Further, with regard to calcium sulfate, its solubility decreases with increase in temperature and therefore the rate of crystallization of calcium sulfate increases more at higher temperatures. This rapid crystallization tends to foul the surface of the membrane, which would definitely lead to a decline in the flux.

#### 4.1.1 SEM & EDX Analysis

The crossflow velocity has been shown to affect the membrane fouling, as seen through the SEM and EDX data in **Figure 4.3**. The initial fouling phases are apparent when the SEM image was captured at an CFV of 8 cm/s revealing the presence of quartz ( $\text{SiO}_2$ ), with minimal calcium carbonate ( $\text{CaCO}_3$ ) using the EDX spectrum. The use of a higher CFV of 16 cm/s results in the deposition of more  $\text{CaCO}_3$  crystals, which can be expressed by the higher density observed in the SEM image and the increased calcium and carbonate peaks in the EDX pattern. At CFV of 24 cm/s, on the SEM image, there is an even denser layer of  $\text{CaCO}_3$ , according to the EDX analysis, fouling is severe due to the high concentration of calcium and carbonate. These results prove that at higher CFVs, the fouling of the membrane due to the deposition of calcium carbonate and other minerals enhances, which decreases the flux performance of the membrane; therefore, the flow characteristics should be managed efficiently to reduce fouling and improve the performance of the most crucial membrane.

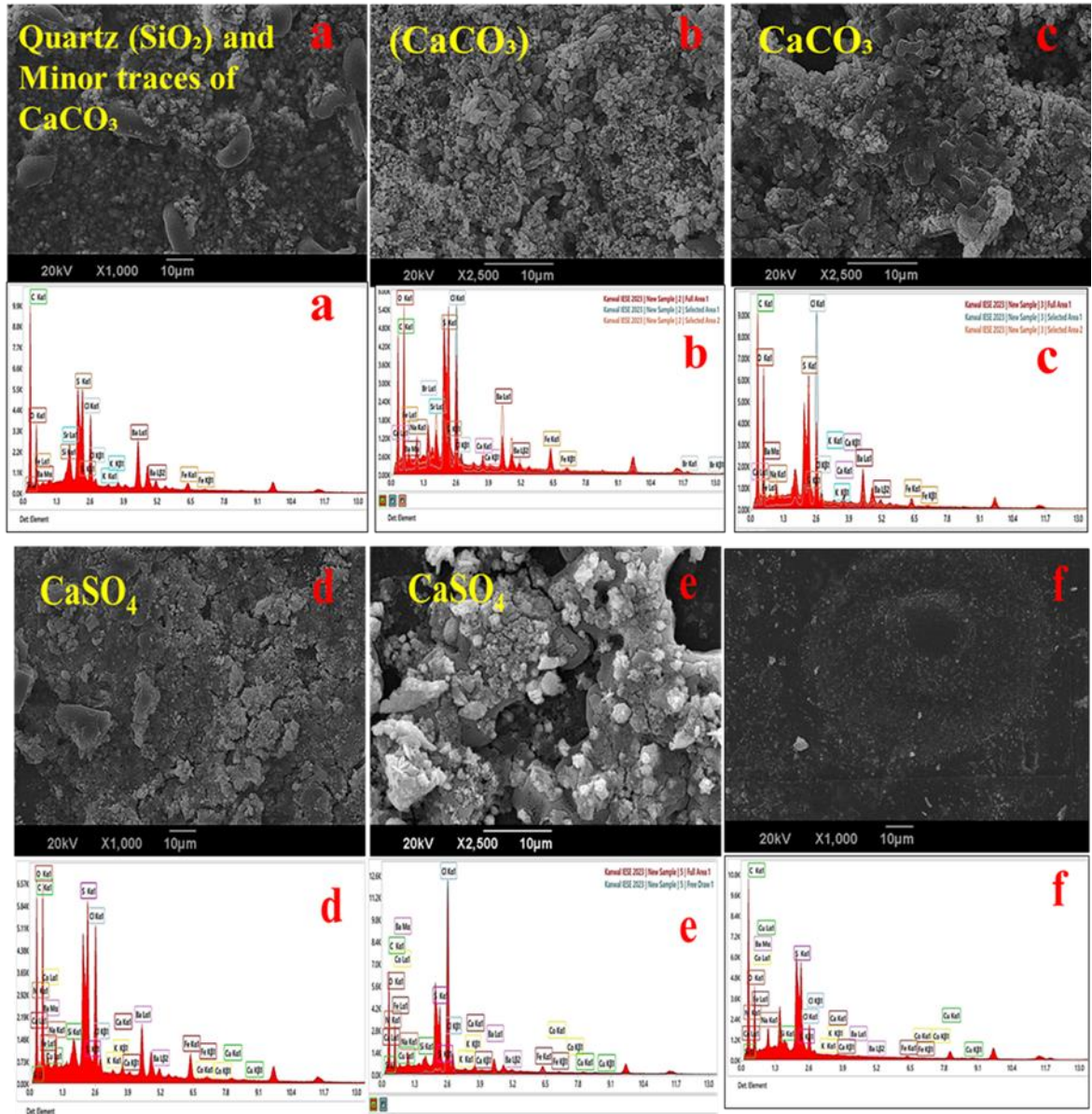


**Figure 4.3:** SEM-EDX analysis of AL of (a) CFV (FS = 8cm/s, DS = 8cm/s @ FS = 25°C, DS = 25°C) (b) CFV (FS = 16cm/s, DS = 8cm/s @ FS = 25°C, DS = 25°C) (c) CFV (FS = 24cm/s, DS = 8cm/s @ FS = 25°C, DS = 25°C) (d) CFV (FS = 8cm/s, DS = 8cm/s @ FS = 40°C, DS = 25°C) (e) CFV (FS = 8cm/s, DS = 8cm/s @ FS = 50°C, DS = 25°C)

SEM and EDX studies helped in understanding the surface roughness and energy dispersive X-ray of the fouling layers present on the active layer of the membrane at different temperatures at a fixed CFV of 8 cm/s for the both the feed solution and the draw

solution. Analyzing the SEM image obtained at 30°C, identified minerals are quartz (SiO<sub>2</sub>) with minor amount of calcium carbonate (CaCO<sub>3</sub>) where EDX spectrum also had peaks for silicon and calcium. The qualitative analysis of the SEM images showed that at 40°C, a more considerable amount of calcium sulfate (CaSO<sub>4</sub>) was deposited at the surface, which was confirmed with increased spectra intensity peaks of calcium and sulfur in the EDX analysis implying change in fouling type. The adverse effect of fouling was more evident at 50°C and showed denser crystal layers of CaSO<sub>4</sub> with more EDX peaks precipitating higher calcium and sulfur content.

Hence, it is evident that high temperatures cause constitutive fouling due to the more deposition of calcium sulfate and other minerals as pointed out that the flux performance decreases with increase in temperature and therefore temperatures should be optimized to reduce fouling and enhance the efficiency of the membrane.

#### *4.1.2 FTIR Analysis*

The FTIR analysis was done for both the fresh membrane and the fouled membranes, which have been rinsed with DI water, to determine any chemical change that the active group of the membrane may have gotten into due to interaction with foulants. The first spectrum can be described as the initial composition of the membrane since there are no significant signs of damage or alteration on the membrane. **Figure 4.4** shows the position of peaks and variation in the intensity level.

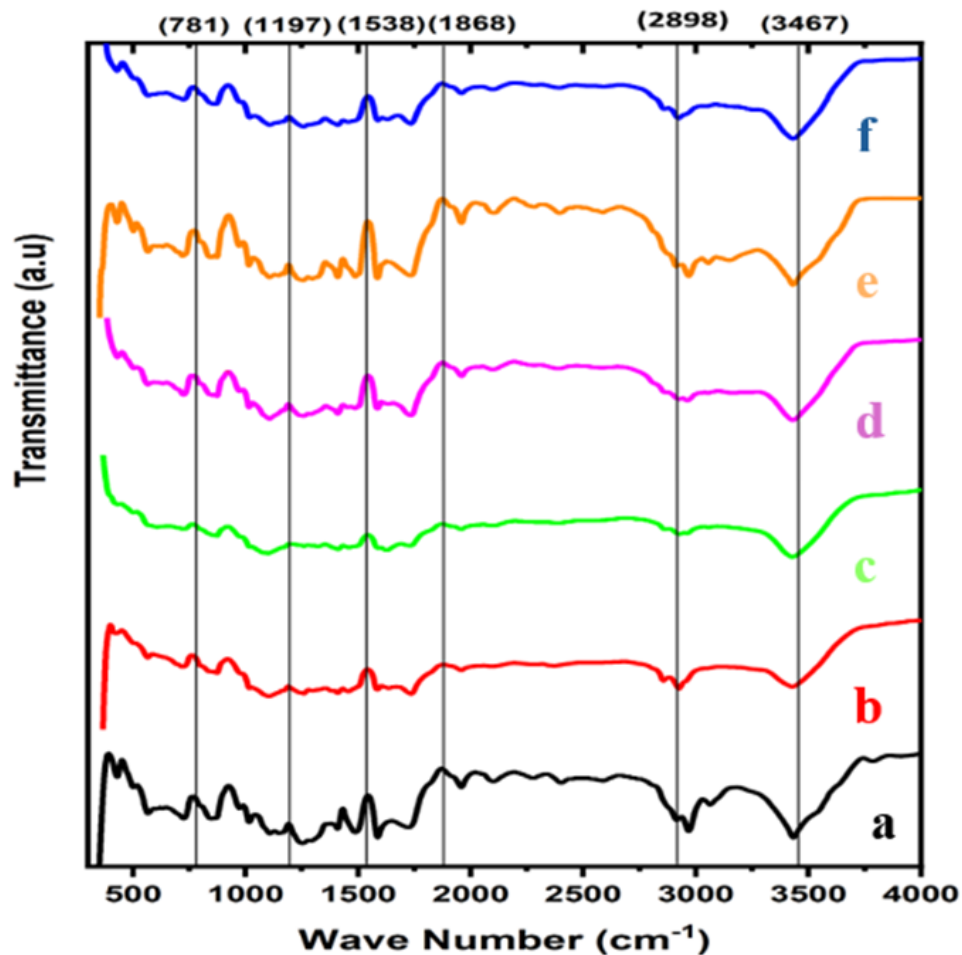


**Figure 4.4:** FTIR Analysis of active layers of (a) pristine membrane (b) CFV (feed solution = 8cm/s, draw solution = 8cm/s) (c) CFV (feed solution = 16cm/s, draw solution = 8cm/s) (d) CFV (feed solution = 24cm/s, DS = 8cm/s) (e) Temperature (feed solution = 40°C, draw solution = 30°C ) (f) (feed solution = 50°C, DS = 30°C )

FTIR spectrum shows the Absorption Bands at definite wavenumbers which ranges from 781, 1197, 1538, 1868, 2898, 3467  $\text{cm}^{-1}$  and is depicted by the various functional groups or molecular bonds. One at 1197  $\text{cm}^{-1}$  it relates them with C-O stretching vibrations. The detailed assignment of the bands is as follows: The band at 1538  $\text{cm}^{-1}$  may be attributed to N-H bending or C=C stretching. For instance, although the one at 1868  $\text{cm}^{-1}$  has been assigned as C=O, and 2898  $\text{cm}^{-1}$  has been assigned to C-H stretching of some functional groups. Finally, the band at 3467  $\text{cm}^{-1}$  may be also attributed to OH or NH stretching

frequency rarely. More importantly, the position and peak intensity of the spectra “a” to “f” have not only shows the position of the peaks but also the variation in the intensity suggesting to this end that there is no interaction between foulant and membrane surface. Therefore, it can be seen that the FO membrane is stable when used for petroleum wastewater reconcentration purpose and the same can be reused several times.

## **4.2 Sulfate Removal via EC**

### *4.2.1 Effect of Current on Sulfate Removal with Stainless Steel Electrodes*

This experiment focuses on the removal of sulfate ion concentration in wastewater using EC with stainless steel electrodes, with respect to the current. The **Figure 4.5** below refers to the percentage of sulfate removal under various flow rates (750 mA, 1000 mA, 1250 mA, 1500 mA) and time duration for an EC batch mode setup equipped with mono-polar series arrangement having stainless steel (SS) electrodes. The residence time was set at levels ranging from 0 to 60 mins. From the given results the maximum efficiency of sulfate removal was recorded at a current of 1500mA and was found to be 21.59% after 60 minutes. This implies that with high current, this removal efficiency is improved probably due to increased formation of coagulants and flocculation mechanisms. When the current was at 1250 mA, the removal efficiency of the sulfate was 15.91% at the end of the experiment. The removal capacity for sulfate of the current 1000 mA was 9.09% at 20 min but reduced with increasing minutes implying that intermediate currents could improve but are not effective in the long run. The degree of removal efficiency was lowest at 750 mA, achieving only 4.55% over the first 30 minutes then gradually decreasing.

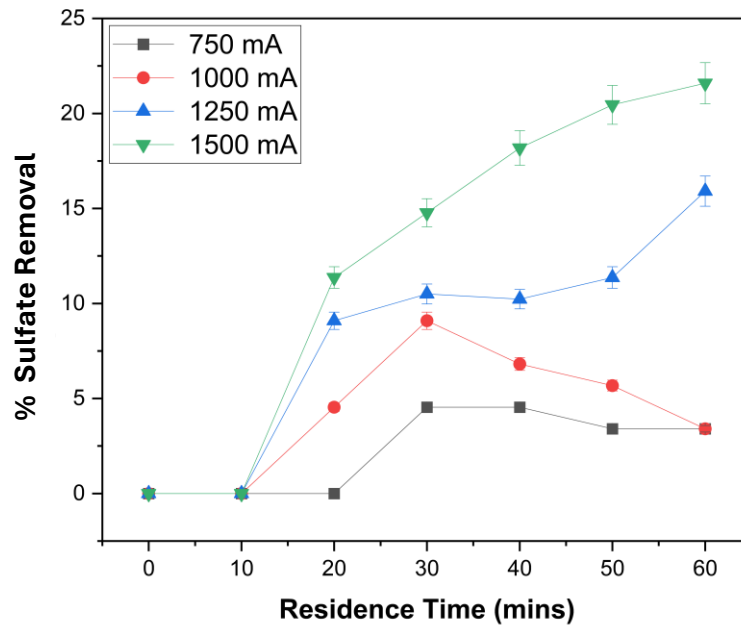


**Figure 4.5:** Effect of current on sulfate removal with stainless steel electrodes with MP-S

#### 4.2.2 Effect of Current on Sulfate Removal with Aluminium Electrodes

The **Figure 4.6** below shows how various current levels (750 mA, 1000 mA, 1250 mA, and 1500 mA) affect the sulfate removal efficiency over time at batch mode EC system using mono-polar series connection and aluminum (Al) electrodes. Similar to the previous setup, the residence time was ranging from 0 to 60 minutes.



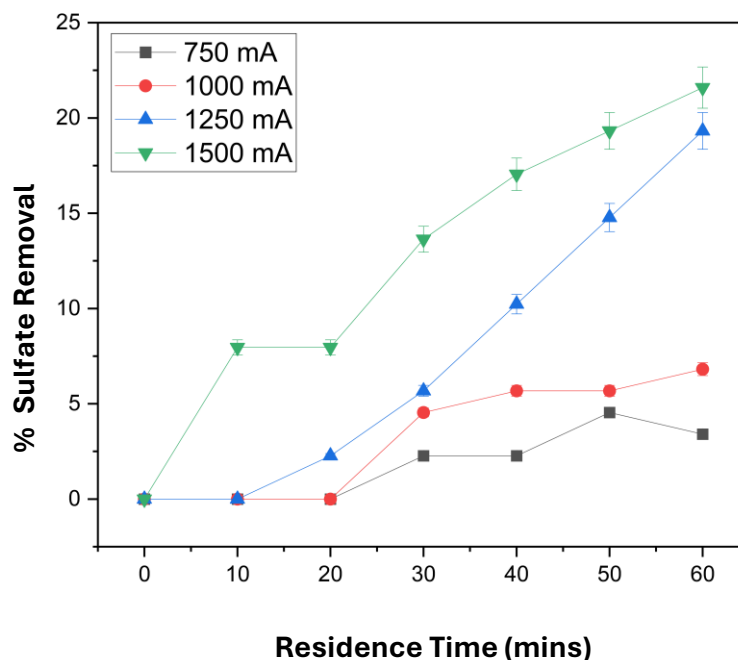


**Figure 4.6:** Effect of current on sulfate removal with aluminium electrodes with MP-S

Again, the maximum removal of sulfate was obtained at a current of 1500 mA which was 21.59% achieved after 60 minutes. At 1250 mA the current, the sulfate removal was somewhat lower at 19.32% at the end of the experiment. The current of 1000 mA gave the moderate electrolysis effect of sulfate ions removal, and it was 6.82% after 60 minutes. To a minimum current of 750 mA the removal efficiency drops to 3.41% sulfate removal at the end of 60 minutes. In conclusion, experiments from both stainless steel and aluminum electrodes depict higher sulfate elimination in the EC process with the increment of current density at 1500 mA.

4.2.3 *Effect of Current on Sulfate Removal with Aluminium Electrodes in Mono-Polar Parallel Arrangement*

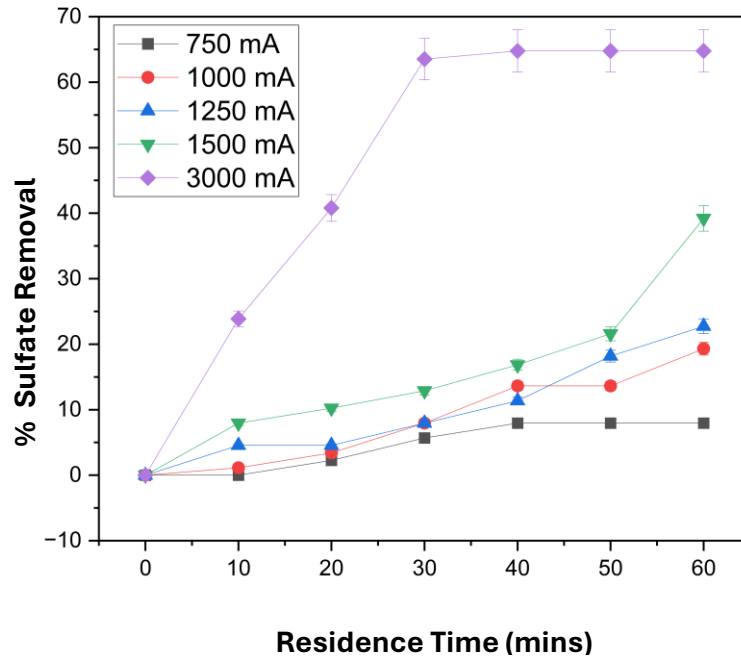


**Figure 4.7** represents the comparison of performance efficiency with the variations in current densities (750 mA, 1000 mA, 1250 mA, 1500 mA and 3000 mA) of the electrocoagulation batch mode setup with mono-polar parallel aluminum electrodes in the removal of sulfate. The residence time was ranging from 0 to 60 minutes.

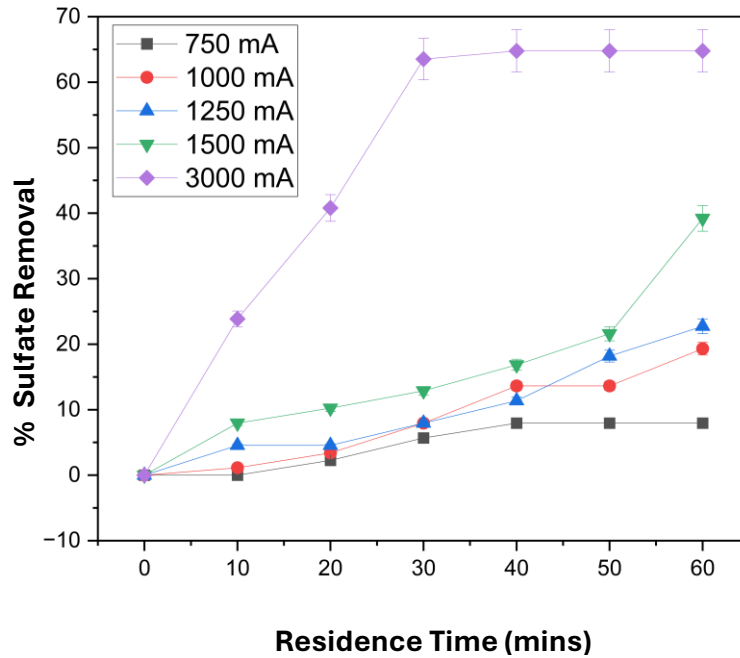


**Figure 4.7:** Effect of current on sulfate removal with aluminium electrodes with MP-P

Sulfate removal efficiency reached its peak at 3000mA of current with an efficiency of 63.52% removal after 60 minutes. As seen from the above results, it is indicated that when current is increased then the coagulant production and the effective flocculation increases, and consequently better sulfate discharge is achieved. And at a current of 1500 mA, sulfate ions present in the solution was removed to the extent of 39.20% after 60 minutes. For the current of 1250 mA the concentration of sulfate ions was decreased to 22.93 % and while the 1000 mA current removing 19.32% of sulfates. The overall aspect of the result indicates that the removal efficiency was the least at 750 mA: amounting to only 7.99% after 60 minutes.

In conclusion, the findings show that the increase in current values enhances sulfate removal efficiency considerably in an EC process of aluminium electrode with parallel

connection. 3000 mA yielded the best results but the balance between energy usage and efficiency toward the removal of sulfates is important in real-life usage.

#### *4.2.4 Effect of Bipolar Arrangement on Sulfate Removal at 1000 mA*

The **Figure 4.8** depicts a comparative use of aluminum and stainless-steel electrodes in the removal of sulfate in an EC batch mode with bipolar configuration with a steady current of 1000 mA. The residence time ranged from 0 to 60 mins. As for sulfate, the findings indicate that a higher removal rate of sulfate ions was recorded in the case of using aluminum electrodes instead of stainless-steel electrodes. Particularly, when indicating the tests with the aluminum electrodes, sulfate removal efficiency was 65.80% in 30 minutes. However, the SS electrodes had a significantly lower efficiency when compared to the other two types of electrodes, with a maximum sulfate removal of only 16.86% at 40 minutes and subsequently decreases slightly.

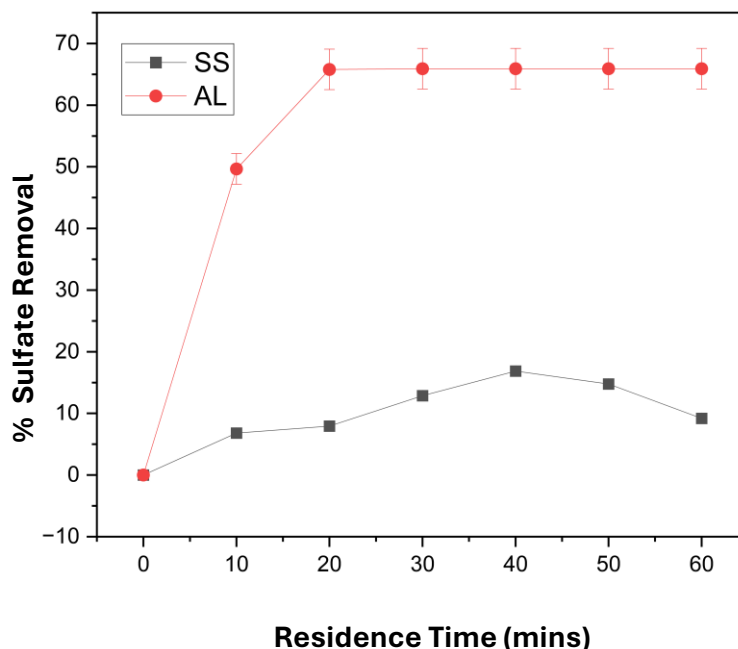


**Figure 4.8:** Effect of bi-polar series arrangement on sulfate removal at 1000 mA

There are a number of reasons which could explain the enhanced performance of aluminum electrodes. The aluminum from the aluminum electrodes when dissolved in the EC process contributes to the formation of different polymeric aluminum hydroxides when ions  $Al^{3+}$  are formed. Hydroxides act as strong coagulants, which are capable of counter act the charge existing on the surface of sulfate ions to coagulate them with other similar charged ions into larger particles, easily separable from the solution. Second, it was observed that the aluminum hydroxides possess high adsorption which contributes to the elimination of sulfate and other impurities.

However, in EC, stainless steel electrodes produce mainly iron hydroxides with trace amounts of other metal ions. Iron hydroxides are also good coagulants; however, their adsorption capacities are usually lower than those of aluminum hydroxides. This leads to less efficient sulfate removal whenever stainless-steel electrodes are used. Also, the

electrochemical nature of the aluminum makes it dissolve better and form coagulant species for enhanced sulfate elimination. The bi-polar arrangement using aluminium electrodes is highly beneficial regarding the removal of sulfate in EC processes and offer a better performance as compared to mono-polar parallel and mono-polar series arrangement, but it need to be check in terms of economic terms too.

### **4.3 Removal of Ca, Mg, Sulfates, and Total Hardness**

#### *4.3.1 Removal of Ca, Mg, Sulfates, and Total Hardness at 1500mA by using MP-S*

The electro-coagulation batch mode experiment was performed using a mono-polar series arrangement of the electrodes with 1500 mA current and 8 no. of aluminum electrodes placed at 1 cm distance. According to the results shown in **Figure 4.9**, the removal of magnesium was highly efficient, and 100 % magnesium removal was observed in all the time intervals selected in the study including 20, 30, 40, 50 and 60 minutes. Sulfate removal was moderate with a maximum of 21.59%, when performed at 50 minutes. Calcium removal was zero with this configuration. Concerning the overall hardness, the experiment demonstrated a gradual trend towards removal efficiency, which was maximum and amounted to 28.31% at 60 minutes.

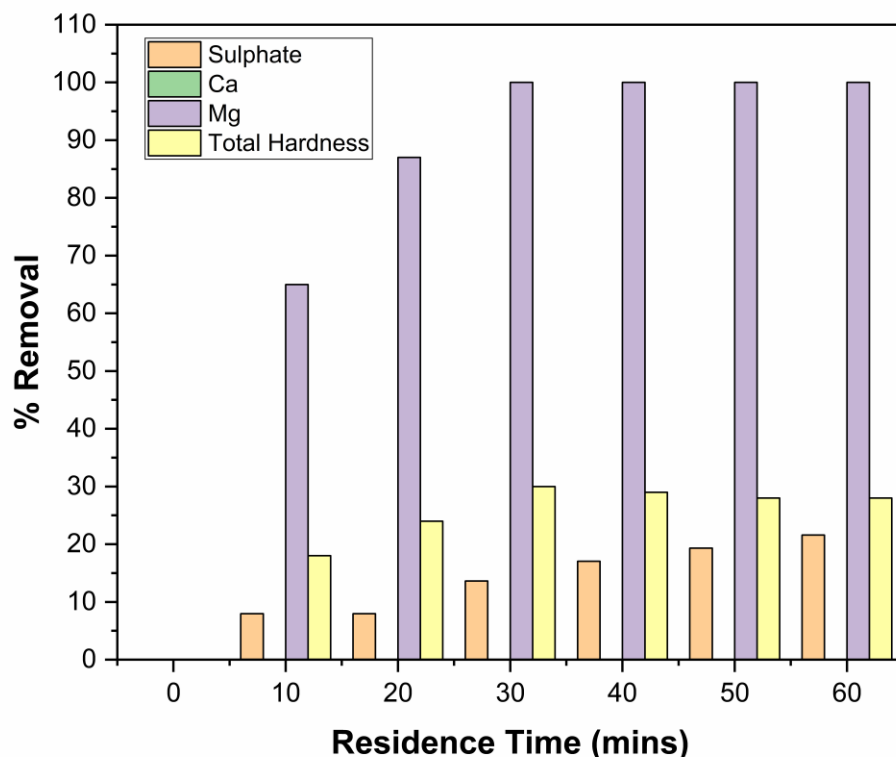


**Figure 4.9:** Removal of Ca, Mg, Sulfates, and Total Hardness at 1500mA by using MP-S

#### 4.3.2 Removal of Ca, Mg, Sulfates, and Total Hardness at 3000mA by using MP-P

This **Figure 4.10** shows the efficiency of calcium, magnesium and sulfates removal and total hardness in electro-coagulation batch mode with mono-polar parallel array at 3000 mA by using aluminium electrode with inter-electrode distance of 1 cm. The removal percentages are depicted with respect to residence time till 60 minutes. First of all, the removal of all ions is characterized by low rates at the beginning. Still, the last few bars, which represent the growing residence time, present a substantial degree of removal.

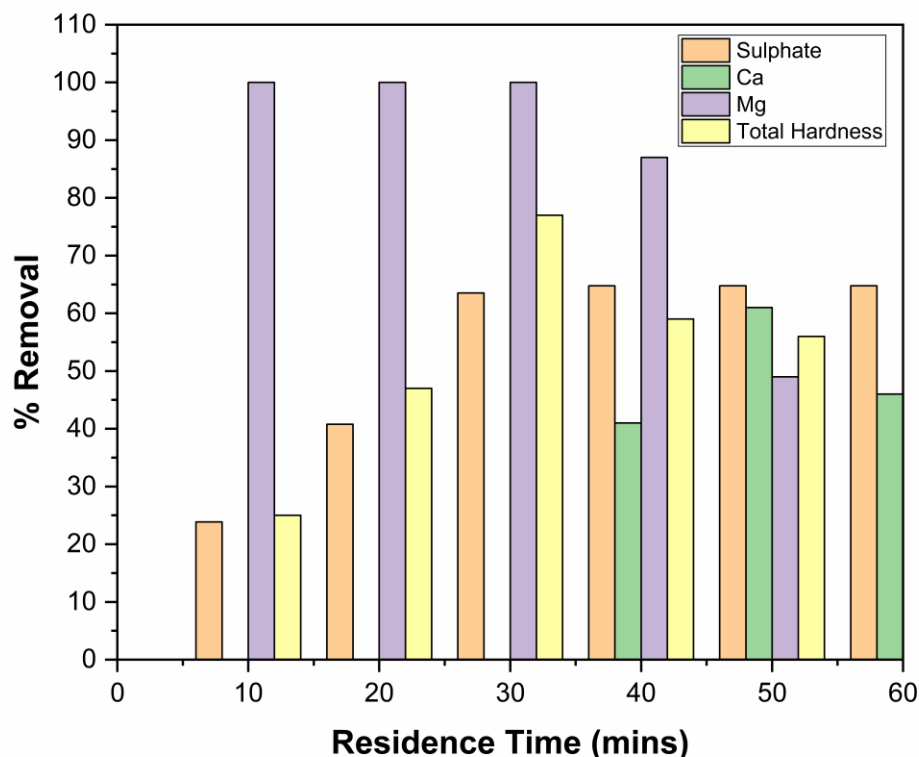


**Figure 4.10:** Removal of Ca, Mg, Sulfates, and Total Hardness at 3000mA by using

MP-P

Magnesium has the highest removal rate, which significantly reached 100% removal at 30 min and was sustained. The maximum removal rate of magnesium may be due to the fact that some of it forms magnesium hydroxide precipitate that is easy to remove by coagulation and flocculation. The electro-coagulation process fosters the production of these hydroxides where they can easily precipitate from the solution. Sulfates with an 87.22% removal rate at 40 minutes. Removal of sulfates is done by precipitation of aluminum hydroxides which react with  $SO_4^{2-}$  and form colloidal complexes which can be easily coagulated. This makes the process have a high removal percentage for sulfate and



thus preferred in the elimination process of sulfate from the wastewater. The results show that the maximum removal of total hardness is 64.77% at 40 minutes and is consistent after that. The main contributor to total water hardness comprises of calcium and magnesium ions, and consequently, the decrease in total hardness is attributed to elimination of these ions. These primary flocs that are produced from the aluminum electrodes work to remove these ions – hence reducing total hardness. Calcium, on the other hand, shows the negative values at the onset of the test suggesting that it can be displaced from the electrode surface but grows to 41.03% at 40 minutes. The negative values of calcium removal at the beginning could be as a result of dissolution of calcium containing compound on the electrode surface. Finally in successive cycles of electro coagulation the calcium ions are flocculated and precipitated as calcium carbonate or calcium hydroxide. The high values of removal rates for magnesium and sulfate mean that there was enhanced coagulation and precipitation by the aid of the aluminum electrodes.

#### *4.3.3 Removal of Ca, Mg, Sulfates, and Total Hardness at 1000mA by using BP-S*

The experiment of electro-coagulation batch mode by using bi-polar series arrangement with aluminum electrode was carried out at 1000 mA, 8-electrodes with interval 1 cm. The experiment was designed to filter calcium (Ca), magnesium (Mg), sulfates, and total hardness from the water. The **Figure 4.11** showed that the effectiveness of the removal of magnesium was high, explicitly achieving 100% at varying time span of 20, 30, 40, 50, and 60 minutes respectively. Sulfate removal fluctuated with the maximum removal efficiency of 65%. The calcium removal was 38.45% observed at 20 minutes. The total hardness removal was also highly fluctuating with the maximum removal efficiency of 65.91% in 30 minutes. In general, the bi-polar series arrangement proved to be highly

effective in the removal of magnesium and capable of minimizing the levels of sulfates and total hardness, although the removal of calcium was comparatively low.

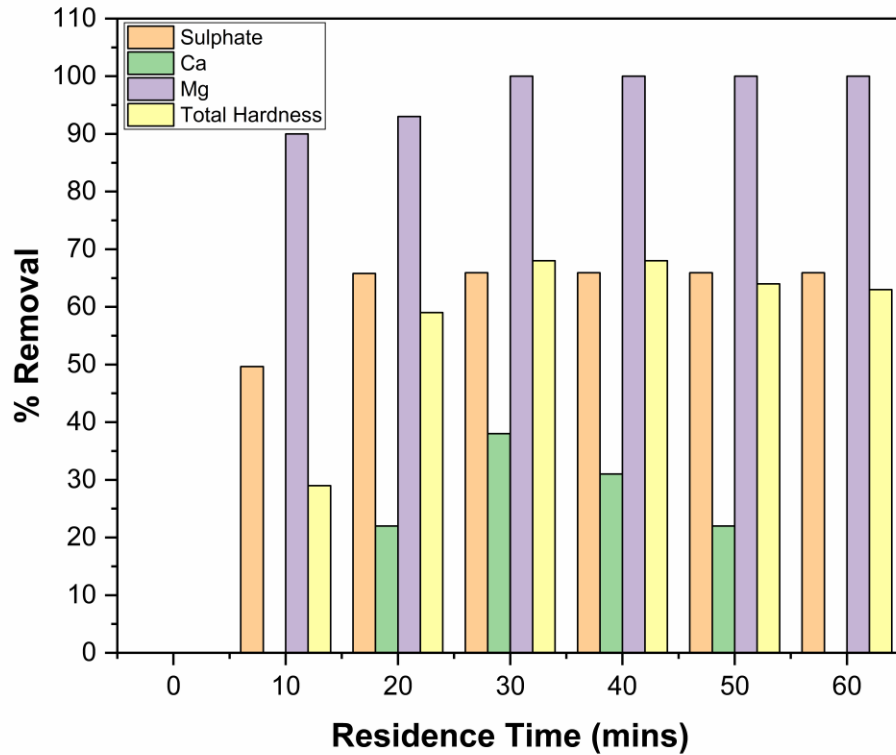


**Figure 4.11:** Removal of Ca, Mg, Sulfates, and Total Hardness at 1000mA by using

BP-S

#### 4.3.4 Impact of Residence time on pH

The **Figure 4.12** illustrates the outcome of an electro-coagulation batch mode experiment in which Al electrodes were used and which investigated the effects of residence time and pH. The experiment was conducted using 8 electrodes of the electrode distance of 1 cm where the current applied was changed. For the current of 1000 mA (BP-S), the pH is

initiated at 8 and gradually rises to 12 upon the completion of the 60 minutes cycling. It suggests a rather drastic alteration in water chemistry as a result of the electro-coagulation process at this particular current. At 3000 mA in MP-P, pH is around 8 in the beginning and increases up to 10 after 60 minutes, hence, the rise in pH is moderate. On the other hand, at 1500 mA (MP-S), the pH is much more stable, which starts at slightly less than 8 up to slightly more than 8 within the 60 minutes.

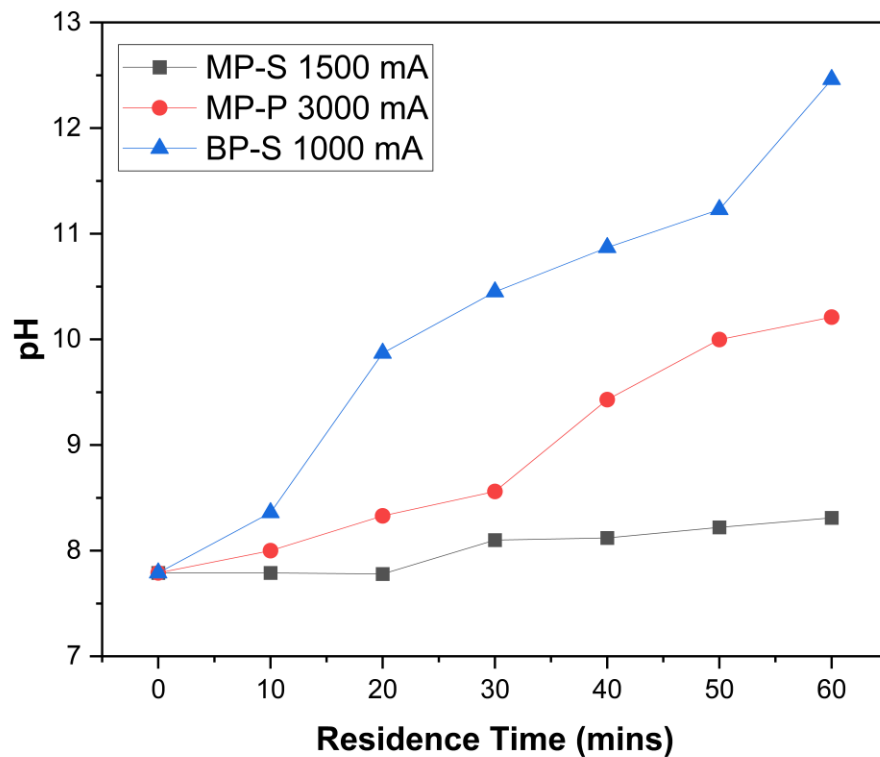


**Figure 4.12:** Impact of Residence time on pH

This reveals that sulfate reduction capability of electro-coagulation processes depends on the pH of the solution. High pH increases the formation of coagulants that help in the

removal of sulfate. The efficiency is considerably lower in an acidic environment (low pH level) due to the scarcity of hydroxide ions.

#### 4.3.5 Electrode Consumption in EC

Electrode consumption is calculated using **Equation 4.1** for all three different arrangements: BP-S, MP-S, and MP-P as shown in **Table 4.2**. For BP-S, operating at a current of 1A and a current density of 8.61 mA/cm<sup>2</sup>, the aluminum consumption was 0.167 g, costing 0.09 PKR. The MP-S arrangement, with a current of 1.5 A and a current density of 12.92 mA/cm<sup>2</sup>, consumed 0.505 g of aluminum, costing 0.28 PKR. The MP-P arrangement, at a current of 3 A and a current density of 25.84 mA/cm<sup>2</sup>, had the highest aluminum consumption of 0.673 g, costing 0.37 PKR. All arrangements used aluminum as the electrode material. The price per gram of aluminum was noted to be 0.557 PKR.

**Table 4.2:** Electrode Consumption in EC

Arrangement	Current (A)	Current Density (mA/cm <sup>2</sup> )	Electrode Material	Electrode Consumption (g/m <sup>3</sup> )	Electrode Price (PKR)
BP-S	1	8.61	Al	0.17	0.09
MP-S	1.5	12.92	Al	0.51	0.28
MP-P	3	25.84	Al	0.67	0.37

Faraday's laws to relates to the amount of electrode consumed, using the formula

**Equation 4.1:** Electrode Consumption in EC

$$m=Q\times M/n\times F$$

where “m” is the mass of aluminum in grams, “Q” is the total charge in Coulombs, “M” is the molar mass of aluminum (approximately 26.98 g/mol), “n” is the number of electrons involved in the reaction (for aluminum, (n=3), and “F” is Faraday's constant (approximately 96485 C/mol). This data indicates that higher current and current density result in increased consumption of aluminum electrodes, leading to higher costs.

*4.3.6 Energy Consumption in EC*

The BP-S arrangement operates at a current of 1 A and a voltage of 31.6 V, with a current density of 8.61 mA/cm<sup>2</sup>. This arrangement consumes 15.8 kWh/m<sup>3</sup> of energy, resulting in an electricity bill of 34.82 PKR as shown in

**Table 4.3.** The MP-S arrangement, with a current of 1.5 A and a voltage of 27.9 V, has a current density of 12.92 mA/cm<sup>2</sup>. This configuration consumes 41.85 kWh/m<sup>3</sup> of energy, leading to an electricity bill of 92.24 PKR. The MP-P arrangement operates at a higher current of 3 A but a much lower voltage of 3.9 V, resulting in a current density of 25.84 mA/cm<sup>2</sup>. This setup consumes 7.8 kWh/m<sup>3</sup> of energy, which translates to an electricity bill of 17.19 PKR. The unit price for electricity is noted to be 22 PKR (\$0.079). The energy consumption of electrode configurations is calculated through **Equation 4.2** where “V” is the voltage applied, “I” is the current and “t” is the reaction time.

**Equation 4.2:** Energy Consumption in EC

$$\text{Energy Consumed}(kWH) = \frac{V * I * t}{1000}$$

**Table 4.3:** Energy Consumption in EC

Arrangement	Current (A)	Voltage V	Current Density (mA/cm <sup>2</sup> )	Energy Consumed (kWh/m <sup>3</sup> )	Electricity Bill (PKR)
BP-S	1	31.6	8.61	15.8	34.82
MP-S	1.5	27.9	12.92	41.85	92.24
MP-P	3	3.9	25.84	7.8	17.19

The data indicates that the MP-P arrangement, despite operating at a higher current, is more energy-efficient and cost-effective compared to the BP-S and MP-S arrangements.

**Impact of Pre-Treatment on FO Flux**

**Figure 4.13** shows that before pre-treatment, the flux starts at approximately 18 LMH and rapidly declines, dropping to around 10 LMH by the 5-hour mark and continuing to decrease. The average flux in this condition is 7.04 LMH. After pre-treatment, the flux begins slightly higher and decreases more gradually. The average flux after pre-treatment is 9.47 LMH. In summary, an increase in the average flux by 7.04 LMH to 9.47 LMH is used to show that the pre-treatment step has helped in improving the efficiency of the FO process. The water flux increased by 35% after the pre-treatment by EC.

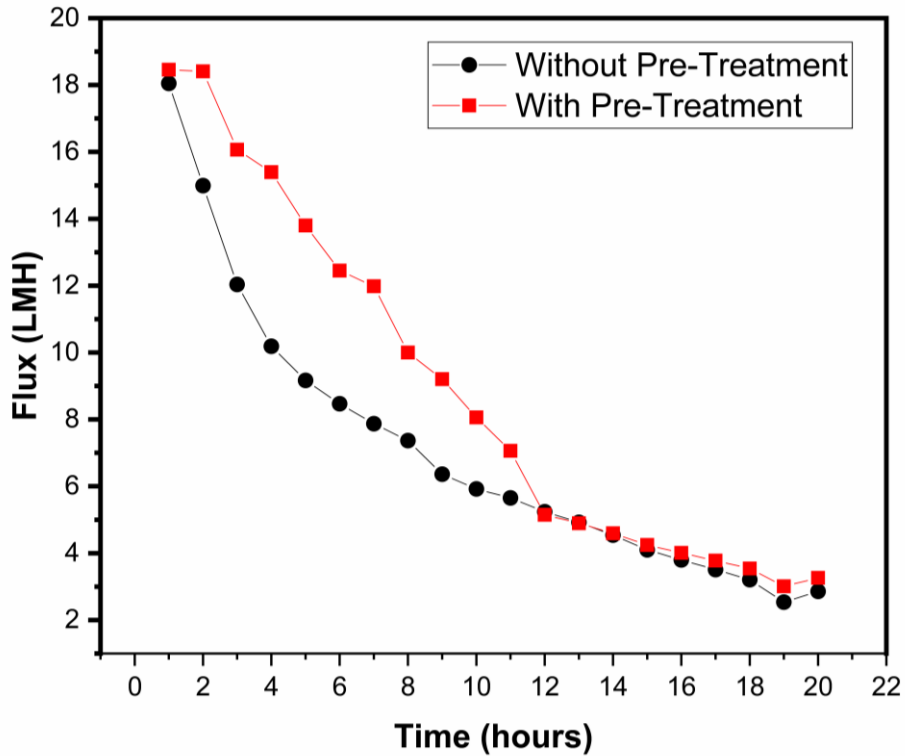


**Figure 4.13:** Impact of Pre-Treatment by electro-coagulation on FO flux

#### 4.4 Flux Comparison for New Membrane, Chemical Cleaning, and Physical Cleaning

The **Figure 4.14** illustrates that the new membrane maintains the highest flux over time, with an average flux of 9.47 LMH. After chemical cleaning, the flux is lower than that of the new membrane but still relatively high, averaging 7.97 LMH. This suggests that chemical cleaning is able to recover much of the permeability of the membrane. However, after physical cleaning, the total flux is substantially lowered in average about 5.28 LMH. This correlation, therefore, indicates that the physical-cleaning approach is less effective in sustaining flux as compared to the chemical-cleanliness approach.

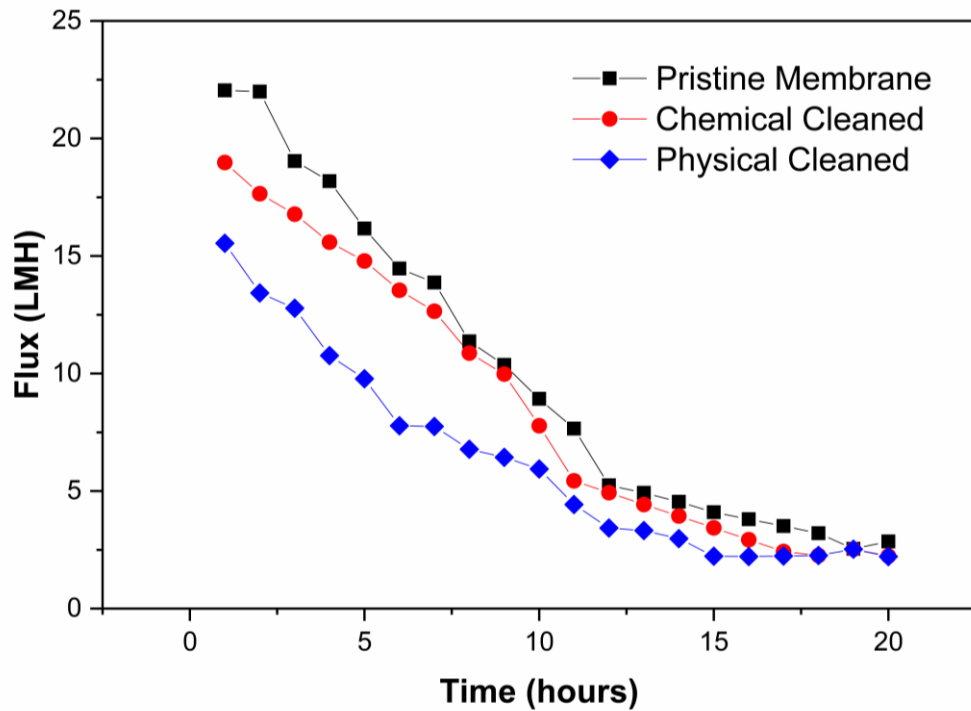


**Figure 4.14:** Flux comparison for new membrane, chemical cleaning, and physical cleaning

Generally, the new membrane shows the best performance, and chemical cleaning demonstrates better performance as compared to physical cleaning which has the worst performance in terms of maintaining the flux.

#### 4.5 Comparative Analysis of Wastewater and Treated Wastewater Parameters

The **Table 4.4** shows a comparative study of different aspects of real, synthetic and treated wastewater with 3000 mA EC. The general parameters show that conductivity and total dissolved solids values are lower in the EC treated water showing the removal of dissolved ions and salts. The pH of the treated wastewater has increased to be alkaline from acidic/neutral which could affect the efficiency of the removal of different pollutants. The



levels of turbidity are lower in the treated water; signifying that they contain lower levels of suspended particles. In the terms of ion concentrations, it can be noted that sodium, potassium, calcium, magnesium, chloride, and sulfate concentrations are all decreased after the EC treatment. The most significant changes have been observed in the decrease of magnesium and sulfate ions, which shows the impressive effectiveness of EC in their removal.

**Table 4.4:** Comparative analysis of wastewater and treated wastewater parameters

<b>Parameters</b>	<b>Samples</b>	<b>Synthetic Final Non-Oily Stream</b>	<b>Treated by EC (MP-P @ 3000 mA)</b>
<b>Conductivity</b>	uS/cm	17,200	13,320
<b>TDS</b>	ppm	11,000	9,770
<b>pH</b>	-	7.79	10.87
<b>Turbidity</b>	NTU	10	3
<b>COD</b>	ppm	20	0
<b>Oil &amp; grease</b>	ppm	20	9.88
<b>TSS</b>	ppm	2	0
<b>Sodium</b>	ppm	2,765	2,256
<b>Potassium</b>	ppm	195	148
<b>Calcium</b>	ppm	580	339
<b>Magnesium</b>	ppm	180	23
<b>Chloride</b>	ppm	6,690	5,245
<b>Sulfate</b>	ppm	676	217.5

In conclusion, the findings of this study demonstrate how electro-coagulation can be useful in the degradation of the different contaminants as well as the enhancement of the general quality of water that is in the wastewater.

#### **4.6 Semi Continuous EC-FO**

The **Figure 4.15** shows the efficiency of a semi-continuous EC-FO process under pre-optimization where the feed was subjected to electro-coagulation. The data presented in the diagram is the comparison of the flux and reverse solute flux (RSF) over time. The average flux achieved after 48 hrs was 18 LMH with 0.17 GMH reverse solute flux value as shown in **Figure 4.15**. The rise in flux is due to the increase in osmotic pressure gradient due to continuous dosing of concentrated TEAB in DS and secondly addition of de-ionized water as the FS reaches 500 mL (Phuntsho et al., 2013).

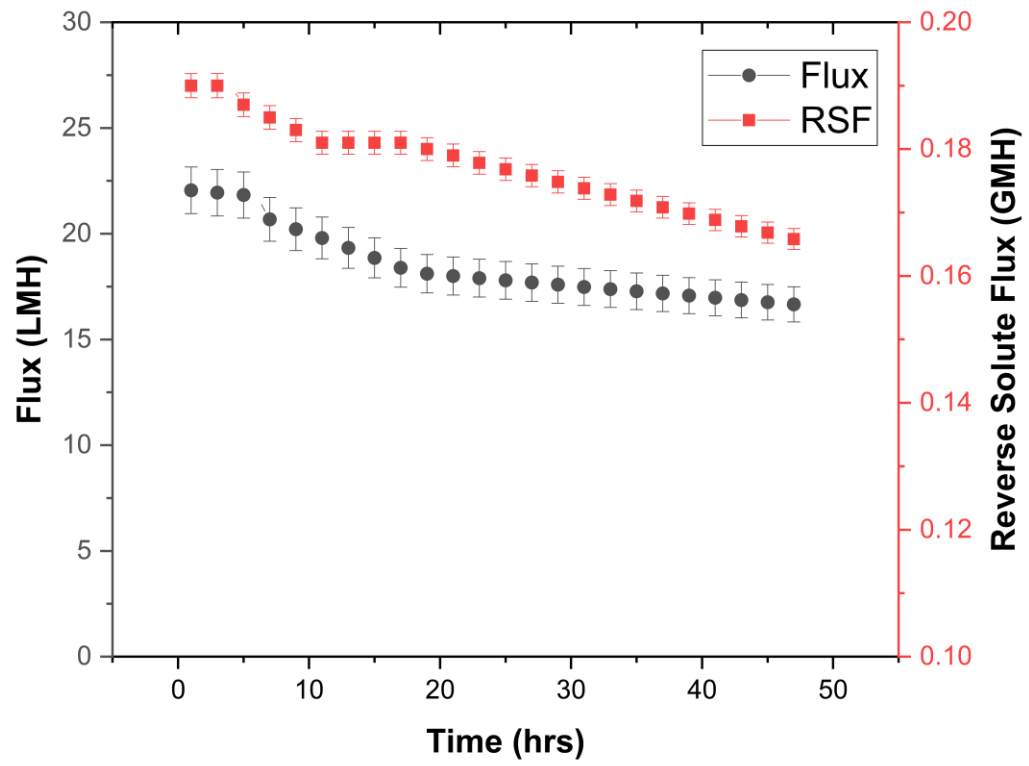


**Figure 4.15:** Semi Continuous EC-FO

## CHAPTER 5: CONCLUSIONS AND RECOMMENDATIONS

### 5.1 Conclusion

This study concluded that the EC-FO system can be used for the pre-treatment and concentration of FNO wastewater streams originating from an oil refinery site. TEAB, a cationic surfactant, was used as a draw solution, which generated a stable 7 LMH flux in the batch experiments without any pre-treatment.  $\text{CaSO}_4$ ,  $\text{CaCO}_3$  and  $\text{SiO}_2$  were found as the key foulants on the FO membrane surface. The interaction of calcium with the polyamide group on the membrane active layer was the main reason for  $\text{CaSO}_4$  scaling. However, the FO membrane depicted a strong chemical resistance against these foulants without any alteration in the structure of its active groups and the thickness of the active layer. These key foulants were targeted in the pre-treatment using EC. After the initial set of optimization experiments, a 1500 mA current was shortlisted for MP-S arrangement, 3000 mA for MP-P arrangement, and 1000 mA for BP-S arrangement with aluminum electrodes. Stainless steel electrodes were not found to be effective in sulfate removal. MP-P arrangement of aluminum electrodes turned out to be the most energy-efficient configuration due to less potential difference across electrodes as the voltage is equally divided across each electrode. At 3000 mA current in MP-P arrangement a 11% reduction in TDS, 41% reduction in calcium, 87% reduction in magnesium and 65% reduction in sulfates is observed. The pre-treated stream produced a 35% higher flux in the forward osmosis process compared to the untreated stream. The FO system showed stability in long-term semi-continuous experiments depicting the suitability of the EC-FO process in practical applications.

## **5.2 Recommendations**

In the present study, it is suggested to incorporate aluminum electrode rather than stainless steel because aluminum electrode has higher removal efficiency for wastewater treatment. To balance the energy consumption with the removal efficiency, it is important to optimize the current density as higher densities yield better results but have to be tested economically. Moreover, it is recommended to arrange MP-P systems to achieve the maximum degree of removal efficiency, especially of sulfates and calcium. All these strategies will contribute to improvement of the general efficiency and economy of the electro-coagulation process.

## REFERENCES

- Abbar, A. H., & Alkurdi, S. S. (2021). Performance Evaluation of a Combined Electrocoagulation– Electrooxidation Process for the Treatment of Petroleum Refinery Wastewater. *IOP Conference Series: Materials Science and Engineering*, 1076(1), 012027. <https://doi.org/10.1088/1757-899x/1076/1/012027>
- Akkaya, G. K. (2022). Treatment of petroleum wastewater by electrocoagulation using scrap perforated (Fe-anode) and plate (Al and Fe-cathode) metals: Optimization of operating parameters by RSM. *Chemical Engineering Research and Design*, 187, 261–275. <https://doi.org/10.1016/J.CHERD.2022.08.048>
- Alamoudi, T., Nawaz, M. S., Obaid, M., Jin, Y., Soukane, S., Son, H. S., Gudideni, V., Al-Qahtani, A., & Ghaffour, N. (2022). Optimization of osmotic backwashing cleaning protocol for produced water fouled forward osmosis membranes. *Journal of Membrane Science*, 663, 121013. <https://doi.org/10.1016/J.MEMSCI.2022.121013>
- Al-Furaiji, M., Benes, N., Nijmeijer, A., & McCutcheon, J. R. (2019). Use of a Forward Osmosis-Membrane Distillation Integrated Process in the Treatment of High-Salinity Oily Wastewater. *Industrial and Engineering Chemistry Research*, 58(2), 956–962. <https://doi.org/10.1021/acs.iecr.8b04875>
- Arcanjo, G. S., Costa, F. C. R., Ricci, B. C., Mounteer, A. H., de Melo, E. N. M. L., Cavalcante, B. F., Araújo, A. V., Faria, C. V., & Amaral, M. C. S. (2020). Draw solution solute selection for a hybrid forward osmosis-membrane distillation module:

- Effects on trace organic compound rejection, water flux and polarization. *Chemical Engineering Journal*, 400, 125857. <https://doi.org/10.1016/J.CEJ.2020.125857>
- Bai, P., Etim, U. J., Yan, Z., Mintova, S., Zhang, Z., Zhong, Z., & Gao, X. (2019). Fluid catalytic cracking technology: current status and recent discoveries on catalyst contamination. *Catalysis Reviews - Science and Engineering*, 61(3), 333–405. <https://doi.org/10.1080/01614940.2018.1549011>
- Cath, T. Y., Childress, A. E., & Elimelech, M. (2006). Forward osmosis: Principles, applications, and recent developments. *Journal of Membrane Science*, 281(1–2), 70–87. <https://doi.org/10.1016/J.MEMSCI.2006.05.048>
- Davarnejad, R., Mohammadi, M., & Ismail, A. F. (2014). Petrochemical wastewater treatment by electro-Fenton process using aluminum and iron electrodes: Statistical comparison. *Journal of Water Process Engineering*, 3(C), 18–25. <https://doi.org/10.1016/j.jwpe.2014.08.002>
- Davood Abadi Farahani, M. H., Borghei, S. M., & Vatanpour, V. (2016). Recovery of cooling tower blowdown water for reuse: The investigation of different types of pretreatment prior nanofiltration and reverse osmosis. *Journal of Water Process Engineering*, 10, 188–199. <https://doi.org/10.1016/J.JWPE.2016.01.011>
- Degnan, T. F. (2015). Chemical reaction engineering challenges in the refining and petrochemical industries - The decade ahead. In *Current Opinion in Chemical Engineering* (Vol. 9, pp. 75–82). Elsevier Ltd. <https://doi.org/10.1016/j.coche.2015.09.003>



- El-Ashtoukhy, E.-S. Z., El-Taweel, Y. A., Abdelwahab, O., & Nassef, E. M. (2013). Treatment of Petrochemical Wastewater Containing Phenolic Compounds by Electrocoagulation Using a Fixed Bed Electrochemical Reactor. In *Int. J. Electrochem. Sci* (Vol. 8). [www.electrochemsci.org](http://www.electrochemsci.org)
- Gągol, M., Przyjazny, A., & Boczkaj, G. (2018). Wastewater treatment by means of advanced oxidation processes based on cavitation – A review. In *Chemical Engineering Journal* (Vol. 338, pp. 599–627). Elsevier B.V. <https://doi.org/10.1016/j.cej.2018.01.049>
- Ghosh, P. (2004). Coalescence of air bubbles at air-water interface. *Chemical Engineering Research and Design*, 82(7), 849–854. <https://doi.org/10.1205/0263876041596715>
- Giwa, S. O., Ertunç, S., Hapoglu, H., Ertunc, S., & Alpbaz, M. (2012). Electrocoagulation treatment of turbid petrochemical wastewater Control of Reactive Distillation Processes View project Electrocoagulation Treatment of Turbid Petrochemical Wastewater. In *International Journal of Advances in Science and Technology* (Vol. 5, Issue 5). <https://www.researchgate.net/publication/304801969>
- Gupta, P., Mondal, S., Gardas, R. L., & Sangwai, J. S. (2022). Investigation on the Effect of Ionic Liquids and Quaternary Ammonium Salts on the Kinetics of Methane Hydrate. *Industrial and Engineering Chemistry Research*. <https://doi.org/10.1021/acs.iecr.2c04595>
- Hamada, M., Ghalwa, N. A., B. Farhat, N., Mahllawi, K. Al, & Jamee, N. (2018). Optimization of Electrocoagulation on Removal of Wastewater Pollutants.

*International Journal of Waste Resources*, 08(04). <https://doi.org/10.4172/2252-5211.1000357>

Jasim, M. A., & Aljaberi, F. Y. (2023). Treatment of oily wastewater by electrocoagulation technology: A general review (2018-2022). In *Journal of Electrochemical Science and Engineering* (Vol. 13, Issue 2, pp. 361–372). International Association of Physical Chemists. <https://doi.org/10.5599/jese.1472>

Jia, X., Jin, D., Li, C., & Lu, W. (2019). Characterization and analysis of petrochemical wastewater through particle size distribution, biodegradability, and chemical composition. *Chinese Journal of Chemical Engineering*, 444–451. <https://doi.org/10.1016/j.cjche.2018.04.030>

Khaing, T. H., Li, J., Li, Y., Wai, N., & Wong, F. S. (2010). Feasibility study on petrochemical wastewater treatment and reuse using a novel submerged membrane distillation bioreactor. *Separation and Purification Technology*, 74(1), 138–143. <https://doi.org/10.1016/j.seppur.2010.05.016>

Khalifa, O., Banat, F., & Hasan, S. W. (2022). Electrochemical treatment of petroleum wastewater: standalone and integrated processes. *Petroleum Industry Wastewater: Advanced and Sustainable Treatment Methods*, 171–183. <https://doi.org/10.1016/B978-0-323-85884-7.00001-1>

Khan, K. A., Zaman, K., Shoukry, A. M., Sharkawy, A., Gani, S., Sasmoko, Ahmad, J., Khan, A., & Hishan, S. S. (2019). Natural disasters and economic losses: controlling external migration, energy and environmental resources, water demand, and financial

- development for global prosperity. *Environmental Science and Pollution Research*, 26(14), 14287–14299. <https://doi.org/10.1007/s11356-019-04755-5>
- Lawson, K. W., & Lloyd, D. R. (1997). Membrane distillation. In *Journal of Membrane Science* (Vol. 124).
- Li, L., Shi, W., Zang, L., Wang, C., & Yu, S. (2020). Factors affecting the performance of forward osmosis treatment for oilfield produced water from surfactant-polymer flooding. *Journal of Membrane Science*, 615, 118457. <https://doi.org/10.1016/J.MEMSCI.2020.118457>
- Luo, Z., Yuan, G., Cen, K., & Li, W. (2022a). Evaluation of the oil-bearing drilling cuttings processing technology in petrochemical industry under cleaner production: A case study in China. *Journal of Cleaner Production*, 375. <https://doi.org/10.1016/j.jclepro.2022.134041>
- Luo, Z., Yuan, G., Cen, K., & Li, W. (2022b). Evaluation of the oil-bearing drilling cuttings processing technology in petrochemical industry under cleaner production: A case study in China. *Journal of Cleaner Production*, 375. <https://doi.org/10.1016/j.jclepro.2022.134041>
- Mark, B. G., Baraer, M., Fernandez, A., Immerzeel, W., Moore, R. D., & Weingartner, R. (2015). Glaciers as water resources. In *The High-Mountain Cryosphere: Environmental Changes and Human Risks* (pp. 184–203). Cambridge University Press. <https://doi.org/10.1017/CBO9781107588653.011>

- Mohammadifakhr, M., Grooth, J. de, Roesink, H. D. W., & Kemperman, A. J. B. (2020). Forward osmosis: A critical review. In *Processes* (Vol. 8, Issue 4). MDPI AG. <https://doi.org/10.3390/PR8040404>
- Moussavi, G., Khosravi, R., & Farzadkia, M. (2011). Removal of petroleum hydrocarbons from contaminated groundwater using an electrocoagulation process: Batch and continuous experiments. *Desalination*, 278(1–3), 288–294. <https://doi.org/10.1016/J.DESAL.2011.05.039>
- Nawaz, M. S., Son, H. S., Jin, Y., Kim, Y., Soukane, S., Al-Hajji, M. A., Abu-Ghdaib, M., & Ghaffour, N. (2021a). Investigation of flux stability and fouling mechanism during simultaneous treatment of different produced water streams using forward osmosis and membrane distillation. *Water Research*, 198. <https://doi.org/10.1016/j.watres.2021.117157>
- Nawaz, M. S., Son, H. S., Jin, Y., Kim, Y., Soukane, S., Al-Hajji, M. A., Abu-Ghdaib, M., & Ghaffour, N. (2021b). Investigation of flux stability and fouling mechanism during simultaneous treatment of different produced water streams using forward osmosis and membrane distillation. *Water Research*, 198. <https://doi.org/10.1016/j.watres.2021.117157>
- Nawi, N. I. M., Bilad, M. R., Anath, G., Nordin, N. A. H., Kurnia, J. C., Wibisono, Y., & Arahman, N. (2020a). The water flux dynamic in a hybrid forward osmosis-membrane distillation for produced water treatment. *Membranes*, 10(9), 1–13. <https://doi.org/10.3390/membranes10090225>

- Nawi, N. I. M., Bilad, M. R., Anath, G., Nordin, N. A. H., Kurnia, J. C., Wibisono, Y., & Arahman, N. (2020b). The water flux dynamic in a hybrid forward osmosis-membrane distillation for produced water treatment. *Membranes*, *10*(9), 1–13. <https://doi.org/10.3390/membranes10090225>
- Orimoloye, I. R., Belle, J. A., & Ololade, O. O. (2021). Drought disaster monitoring using MODIS derived index for drought years: A space-based information for ecosystems and environmental conservation. *Journal of Environmental Management*, *284*. <https://doi.org/10.1016/j.jenvman.2021.112028>
- Padaki, M., Surya Murali, R., Abdullah, M. S., Misdan, N., Moslehyani, A., Kassim, M. A., Hilal, N., & Ismail, A. F. (2015). Membrane technology enhancement in oil-water separation. A review. In *Desalination* (Vol. 357, pp. 197–207). Elsevier. <https://doi.org/10.1016/j.desal.2014.11.023>
- Pérez, L. S., Rodriguez, O. M., Reyna, S., Sánchez-Salas, J. L., Lozada, J. D., Quiroz, M. A., & Bandala, E. R. (2016). Oil refinery wastewater treatment using coupled electrocoagulation and fixed film biological processes. *Physics and Chemistry of the Earth, Parts A/B/C*, *91*, 53–60. <https://doi.org/10.1016/J.PCE.2015.10.018>
- Phuntsho, S., Sahebi, S., Majeed, T., Lotfi, F., Kim, J. E., & Shon, H. K. (2013). Assessing the major factors affecting the performances of forward osmosis and its implications on the desalination process. *Chemical Engineering Journal*, *231*, 484–496. <https://doi.org/10.1016/J.CEJ.2013.07.058>

- Rubio-Clemente, A., Chica, E., & Peñuela, G. A. (2015). Petrochemical wastewater treatment by photo-fenton process. *Water, Air, and Soil Pollution*, 226(3). <https://doi.org/10.1007/s11270-015-2321-x>
- Sahebi, S., Sheikhi, M., Ramavandi, B., Ahmadi, M., Zhao, S., Adeleye, A. S., Shabani, Z., & Mohammadi, T. (2020). Sustainable management of saline oily wastewater via forward osmosis using aquaporin membrane. *Process Safety and Environmental Protection*, 138, 199–207. <https://doi.org/10.1016/J.PSEP.2020.03.013>
- Santos, P. G., Scherer, C. M., Fisch, A. G., & Rodrigues, M. A. S. (2020). Petrochemical wastewater treatment: Water recovery using membrane distillation. *Journal of Cleaner Production*, 267, 121985. <https://doi.org/10.1016/J.JCLEPRO.2020.121985>
- Saqib Nawaz, M., Alamoudi, T., Soukane, S., Soo Son, H., Jin, Y., Medina, S. C., Mustakeem, M., Gudideni, V., Al-Qahtani, A., & Ghaffour, N. (2022). Performance and implications of forward osmosis-membrane distillation hybrid system for simultaneous treatment of different real produced water streams. *Chemical Engineering Journal*, 450, 138479. <https://doi.org/10.1016/J.CEJ.2022.138479>
- Saqib Nawaz, M., Alqulayti, A., Torres Serrano, V. M., Soukane, S., Gudideni, V., Al-Qahtani, A., Yan, I. C., & Ghaffour, N. (2024). Optimizing electrocoagulation pre-treatment efficiency during simultaneous treatment of different produced water streams in a FO-MD hybrid system. *Separation and Purification Technology*, 336. <https://doi.org/10.1016/j.seppur.2024.126290>

- Sardari, K., Fyfe, P., Lincicome, D., & Wickramasinghe, S. R. (2018). Aluminum electrocoagulation followed by forward osmosis for treating hydraulic fracturing produced waters. *Desalination*, 428, 172–181.  
<https://doi.org/10.1016/j.desal.2017.11.030>
- Saththasivam, J., Loganathan, K., & Sarp, S. (2016). An overview of oil-water separation using gas flotation systems. In *Chemosphere* (Vol. 144, pp. 671–680). Elsevier Ltd.  
<https://doi.org/10.1016/j.chemosphere.2015.08.087>
- Shaffer, D. L., Werber, J. R., Jaramillo, H., Lin, S., & Elimelech, M. (2015). Forward osmosis: Where are we now? *Desalination*, 356, 271–284.  
<https://doi.org/10.1016/J.DESAL.2014.10.031>
- Shan, S., Liu, H., Yue, Y., Shi, G., & Bao, X. (2016). Trimetallic WMoNi diesel ultra-deep hydrodesulfurization catalysts with enhanced synergism prepared from inorganic–organic hybrid nanocrystals. *Journal of Catalysis*, 344, 325–333.  
<https://doi.org/10.1016/J.JCAT.2016.09.019>
- Sun, P., Elgowainy, A., Wang, M., Han, J., & Henderson, R. J. (2018). Estimation of U.S. refinery water consumption and allocation to refinery products. *Fuel*, 221, 542–557.  
<https://doi.org/10.1016/j.fuel.2017.07.089>
- Veleva, I., Vanoppen, M., Hitsov, I., Phukan, R., Wyseure, L., Dejaeger, K., Cornelissen, E. R., & Verliefde, A. R. D. (2021). Selection of membranes and operational parameters aiming for the highest rejection of petrochemical pollutants via membrane

distillation. *Separation and Purification Technology*, 259, 118143.  
<https://doi.org/10.1016/J.SEPPUR.2020.118143>

Wang, Q., Liang, J., Zhang, S., Yoza, B. A., Li, Q. X., Zhan, Y., Ye, H., Zhao, P., & Chen, C. (2020a). Characteristics of bacterial populations in an industrial scale petrochemical wastewater treatment plant: Composition, function and their association with environmental factors. *Environmental Research*, 189.  
<https://doi.org/10.1016/j.envres.2020.109939>

Wang, Q., Liang, J., Zhang, S., Yoza, B. A., Li, Q. X., Zhan, Y., Ye, H., Zhao, P., & Chen, C. (2020b). Characteristics of bacterial populations in an industrial scale petrochemical wastewater treatment plant: Composition, function and their association with environmental factors. *Environmental Research*, 189.  
<https://doi.org/10.1016/j.envres.2020.109939>

Wang, X., Xu, H., Zou, Y., Hu, W., & Wang, L. (2022). Mechanistic insight into separation of benzene and cyclohexane by extractive distillation using deep eutectic solvent as entrainer. *Journal of Molecular Liquids*, 368.  
<https://doi.org/10.1016/j.molliq.2022.120780>

Wang, Z., Tang, J., Zhu, C., Dong, Y., Wang, Q., & Wu, Z. (2015). Chemical cleaning protocols for thin film composite (TFC) polyamide forward osmosis membranes used for municipal wastewater treatment. *Journal of Membrane Science*, 475, 184–192.  
<https://doi.org/10.1016/J.MEMSCI.2014.10.032>



- Wei, X., Zhang, S., Sun, Y., & Brenner, S. A. (2018). Petrochemical Wastewater and Produced Water. *Water Environment Research*, 90(10), 1634–1647. <https://doi.org/10.2175/106143018x15289915807344>
- Yan, L., Ma, H., Wang, B., Wang, Y., & Chen, Y. (2011). Electrochemical treatment of petroleum refinery wastewater with three-dimensional multi-phase electrode. *Desalination*, 276(1–3), 397–402. <https://doi.org/10.1016/J.DESAL.2011.03.083>
- Yan, L., Wang, Y., Li, J., Ma, H., Liu, H., Li, T., & Zhang, Y. (2014). Comparative study of different electrochemical methods for petroleum refinery wastewater treatment. *Desalination*, 341(1), 87–93. <https://doi.org/10.1016/j.desal.2014.02.037>
- Yasmeen, M., Nawaz, M. S., Khan, S. J., Ghaffour, N., & Khan, M. Z. (2023). Recovering and reuse of textile dyes from dyebath effluent using surfactant driven forward osmosis to achieve zero hazardous chemical discharge. *Water Research*, 230, 119524. <https://doi.org/10.1016/J.WATRES.2022.119524>
- Yavuz, Y., Koparal, A. S., & Öğütveren, Ü. B. (2010). Treatment of petroleum refinery wastewater by electrochemical methods. *Desalination*, 258(1–3), 201–205. <https://doi.org/10.1016/j.desal.2010.03.013>
- Ye, H., Liu, B., Wang, Q., How, Z. T., Zhan, Y., Chelme-Ayala, P., Guo, S., Gamal El-Din, M., & Chen, C. (2020). Comprehensive chemical analysis and characterization of heavy oil electric desalting wastewaters in petroleum refineries. *Science of the Total Environment*, 724. <https://doi.org/10.1016/j.scitotenv.2020.138117>

Yoo, K., Kashfi, R., Gopal, S., Smirniotis, P. G., Gangoda, M., & Bose, R. N. (2003).  
TEABr directed synthesis of ZSM-12 and its NMR characterization. *Microporous and  
Mesoporous Materials*, 60(1–3), 57–68. [https://doi.org/10.1016/S1387-  
1811\(03\)00317-2](https://doi.org/10.1016/S1387-1811(03)00317-2)